International
Progress Report

IPR-00-34

Äspö Hard Rock Laboratory

TRUE Block Scale Project

Tracer test stage

March'00 structural and hydraulic model based on borehole data from KI0025F03

Jan Hermansson
Thomas Doe

Golder Associates Inc

March 2000

Svensk Kärnbränslehantering AB
Swedish Nuclear Fuel
and Waste Management Co
Box 5864
SE-102 40 Stockholm Sweden
Tel 08-459 84 00
+46 8 459 84 00
Fax 08-661 57 19
+46 8 661 57 19

Äspö Hard Rock
Laboratory

Report no.
IPR-00-34
No.
F56K
Author
Jan Hermanson
Thomas Doe
Date
March 2000
Checked by
Anders Winberg
Date
Dec 2000
Approved
Olle Olsson
Date
Dec 2000

Äspö Hard Rock Laboratory

TRUE Block Scale Project
Tracer test stage

March'00 structural and hydraulic model based on borehole data from KI0025F03

Jan Hermanson
Thomas Doe

Golder Associates Inc

March 2000

Keywords: hydraulic, hydro-structural model, KI0025F03, pressure responses, reconciliation, structural

Table of contents

List of Figures

List of Tables

1 Introduction

This report presents an update of the structural model of the TRUE Block Scale experimental volume based on the drilling of borehole KI0025F03 through the centre of the block.

The iterative process of updating the structural geological model of the block is an ongoing process, which has previously been presented in three technical notes. The first model was based on the drillings of KA2563A and KA3510A and was reported by Hermanson and Follin (1997). Subsequent updates have been presented in the October 1997 model by Hermanson (1997) and in the September 1998 model by Hermanson (1998). The last structural model update was presented in Hermanson (2000) with a hydraulic reconciliation of the conductive structures by Doe (2000).

This report concentrates on borehole KI0025F03 and will only refer to investigations done previously in the block. All defined deterministic structures in the model are presented in this report for completeness and easy accessibility although only a few have changed and two additional structures has been added. The methodology for updating the structural model is presented in **Figure 1-1**.

The following data have been utilised for the KI0025F03 structural model update;

- BIPS/Boremap data of KI0025F03 (CD-ROM 981009)
- POSIVA flowlog of boreholes KI0025F03 (Rouhianien and Heikkinen, 1999)

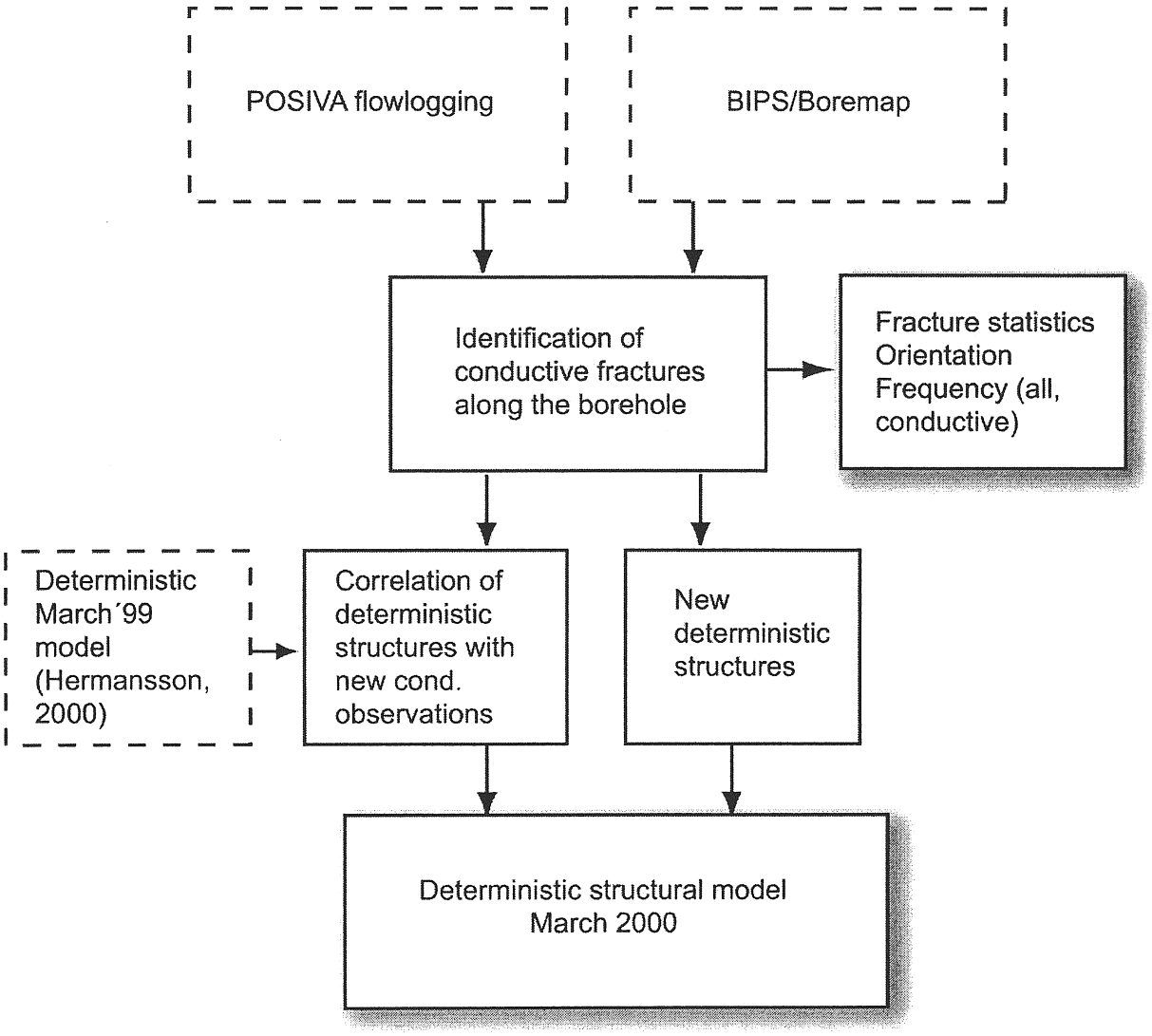

Fig 1-1. *Methodology for updating the structural model*

2 Data sources

2.1 BIPS/Boremap data in KI0025F03

The characterisation of KI0025F03 has been performed using the Boremap system which includes data for rock types and discontinuities. The location, orientation and length of the borehole is given in Table 2-1. The borehole is more or less parallel and drilled in-between boreholes KI0025F and KI0023B. The maximum distances between these two boreholes varies between less than 2 m at the collar to 47 m (KI0025F) and 96 m (KI0023B) at the end of the borehole.

Table 2-1. Borehole data for KI0025F03

KI0025F02	
Collar coordinates	
Easting (m)	1951.848
Northing (m)	7238.868
Elevation (m)	-448.077
Direction	
Bearing (deg)	206.71
Inclination (deg)	-29.17

The lithology of the rock block is given in **Figure 2-1** and is dominated by diorite intersected by small sections of fine-grained granite. Greenstone is observed scattered as minor fragments in the diorite at depth. The origin of the greenstone is uncertain, but surface observations has been interpreted as longer semi-continuous layers of greenstone that might form steep folds in the diorite (Munier, 1995). The main orientation of the greenstone sheets are parallel to the NNE foliation of the rock mass. The fine grained granite is also interpreted to follow the general trend of the greenstone, at least when present. The rock types in the investigated borehole do not differ from what is generally observed in the other boreholes.

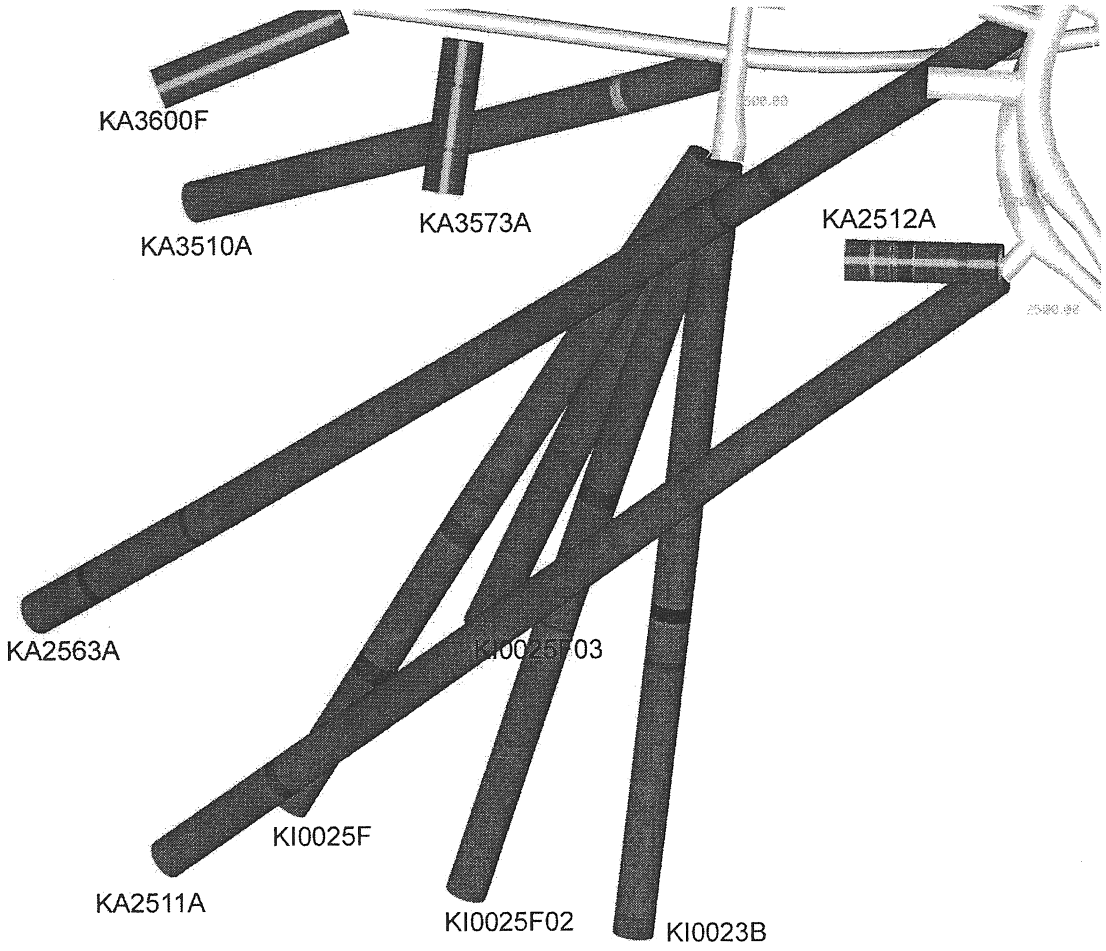

Figure 2-1. *Lithology of the TRUE block scale boreholes.*

KI0025F03 exhibits intense fracturing in the sections between 50 to 60 m and 84 to 100 m. These sections do not necessarily correspond to high inflow. The intensity of fracturing in KI0025F03 is very similar to that observed in KI0025F02, both in respect to position and intensity. However, both boreholes deviates from what is found in KI0025F, just to the east of KI0025F02, which has large sections comparatively unfractured rock. As the distance between the two boreholes KI0025F03 and KI0025F is a maximum of 51 m at the end of the boreholes, the difference in brittle behaviour implies that the fracturing is divided into different domains, one which is more fractured than the other. This difference must lie east of KI0025F02 as fracturing is similar in KI0025F02 and F03. The maximum distance between KI0023F03 to KI0025F02 is approximately 23 m. The average complete fracture frequency is around 2 fractures per meter which is equivalent with observations in KI0025F02.

Orientations of fractures along KI0025F03 reveals two dominant fracture sets, steep northwesterly trending fractures and subhorizontal fractures. There exists a weak northeasterly fracture set that is equivalent with the fracturing observed in KI0025F, KI0025F02 and KI0023B. This pattern is common throughout the HRL (Munier 1995, Hermansson 1998, Rhén et al (1997). Fractures mapped as open constitute approximately 40% of the total amount of fractures and show a pattern which is similar to that of all fractures, cf. **Figure 2-2**, but are more pronounced in the northwesterly direction..

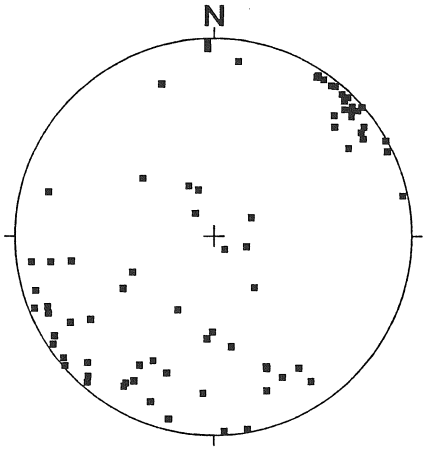

Figure 2-2. *Fracture orientations of all fractures in KI0025F03 plotted as poles to fracture planes on a lower hemisphere equal area projection.*

2.2 The POSIVA flow log and its correlation to conductive fractures in KI0025F03.

POSIVA flow logging has previously been performed in boreholes KI0025F02, KA2563A, KA3510A and KA2511A. Borehole KI0025F03 has also been completely covered by this logging method. The complete logs of all boreholes are published by Rouhianen et al. (1999) and will not be presented here. However, parts of the flow log of KI0025F03 is reproduced in **Figure 2-3** to illustrate the methodology behind identifying highly conductive fractures in the log.

The location is assessed by identifying peak inflow in the borehole. A certain amount of water seeps through as the packers are moved along the borehole and results in a background flow noise in the log. Only peaks do correspond to discrete inflow points. To estimate the conductive fracture frequency along the borehole, inflow points with a sufficiently large inflow were coupled to fractures along the borehole. Conductive fractures were identified in sections with substantial inflow above the background noise. Eighty-three inflow points were coupled to fractures by correlating the bore-map database of natural fractures with the significant inflow points. The threshold value in inflow for identifying conductive fractures varies between 100 to 650000 ml/hr depending on how well a single inflow point stands out from the background noise. If a lower threshold value for inflow was to be chosen more inflow points and consequently more conductive fractures would be identified. Whatever threshold value to use is coupled to the need of resolution when using the data for designing a particular numerical model. From a structural-hydraulic conceptual model point of view it is considered well enough to locate the largest conductive structures of the block with the assumption that less conductive fractures behaves in a similar structural manner. A comparison with the complete fracture data set does not show any major differences in structural behaviour from this subset. Out of the eighty-three identified inflow points, seven structures where connected deterministically between two or more boreholes in the experimental volume. That means that 10% of all flowing features in this borehole were handled as deterministic features, which intersect the other boreholes. The basis

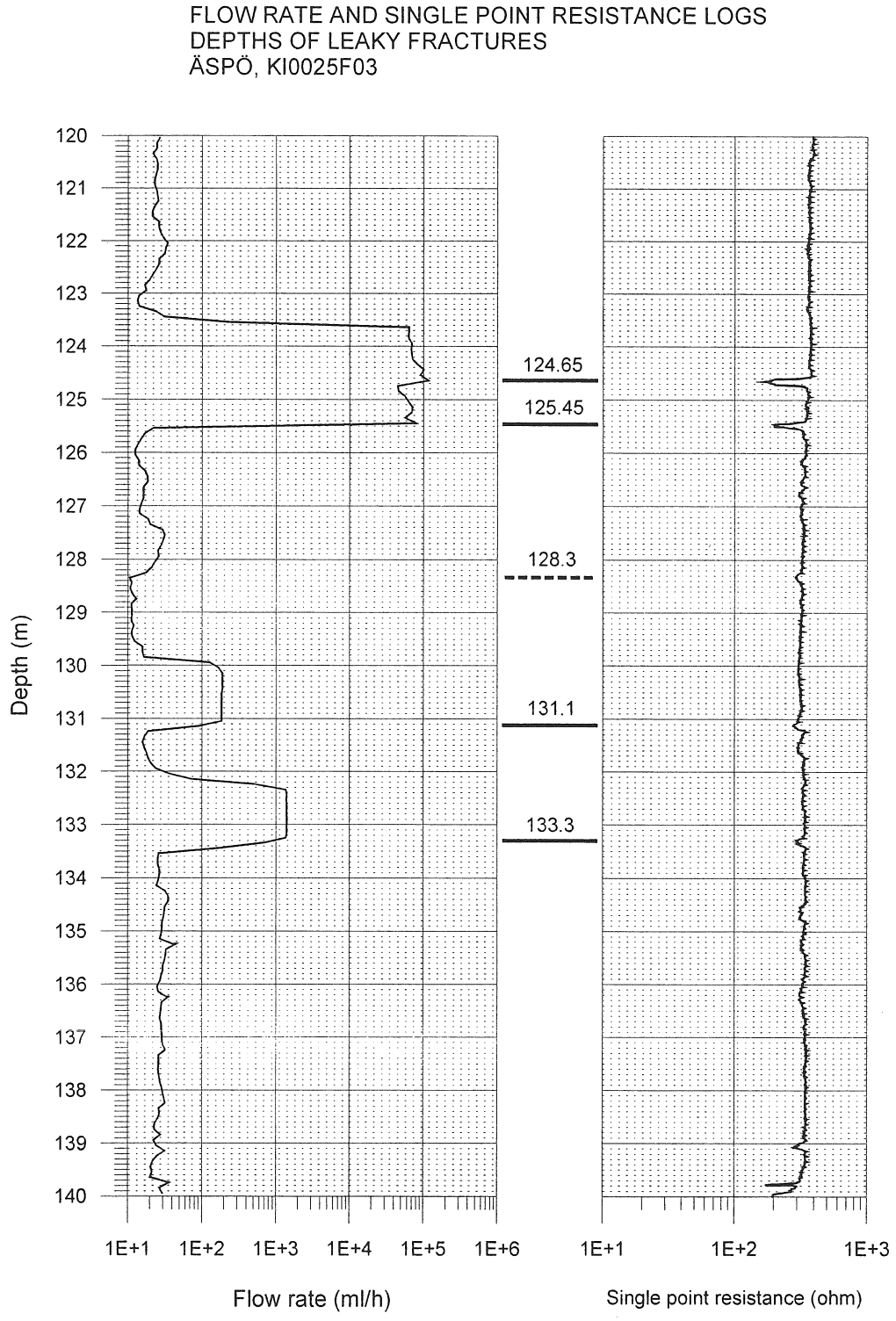

Figure 2-3 *Example of the POSIVA flow log of KI0025F03, section 120 to 140 m from Rouhianen et al. (1999).*

for this choice is directly coupled to drilling responses during the drilling of the borehole but also to flow and transport-tests in-between the boreholes.

Figure 2-4 shows the conductive fracture frequency of borehole KI0025F03 based on the BIPS/POSIVA flow log correlation. The average frequency of conductive fractures

is similar between the boreholes KA2563A, KA2511A, KI0025F and KA3510A and suggests that the major flow paths in the network occur in a distinct proportion of the fracture network, with little variations throughout the investigated part of the block. However, as KI0025F shows large difference to this behaviour with large dry parts of the borehole, the properties of the individual flow paths may be heterogeneous throughout the block

The identified conductive fractures based on the POSIVA flow log is given in Appendix B for reference. The average conductive fracture frequency is 0.62 fractures per metre (compared to the frequency of all fractures which is 2 fractures per metre).

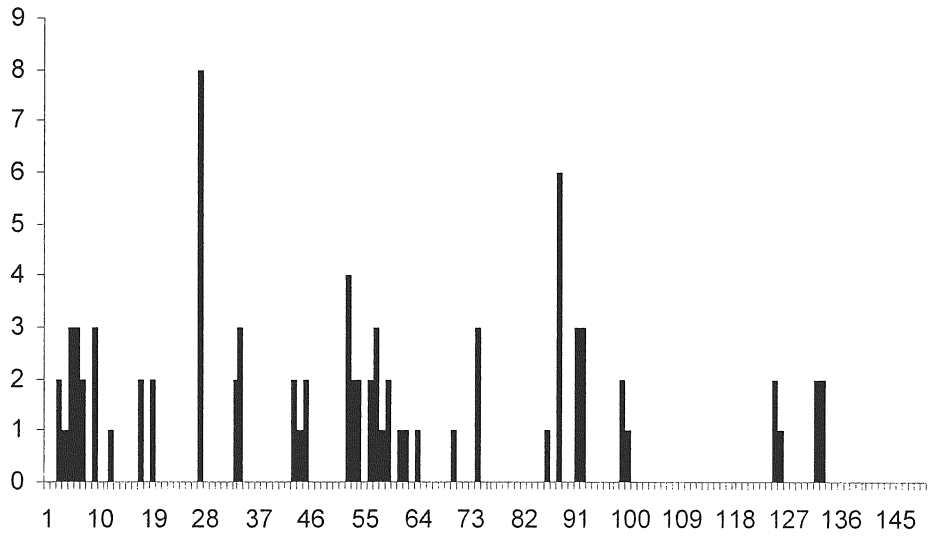

Figure 2-4 *Conductive fracture frequency of borehole KI0025F03 based on the inflow points from the POSIVA flow log and corresponding fractures in these sections.*

The simplified fracture classification presented by Hermanson (1998) has not been extensively utilised when doing the identification of possible conductive fractures in this borehole. The classification had its origin at the time when only 5 m packer tests existed in the boreholes, forcing the geologist to make a qualified guess which fracture within one 5 m section that was conductive. The classification has now become somewhat obsolete with the extensive usage of the POSIVA flow log equipment. It is now in most cases possible to identify exactly the fracture or the fractures that conducts water within a 10 cm section. Nonetheless, the individual geological character of each intercept is still analysed as this is fundamental to the understanding of the geological characteristics of the conductors. Based on previous analyses (Hermanson 2000) the coupling to geologically defined fracture type and inflow is not direct and can thus be somewhat misleading. Hermanson (2000) showed that less than 40% of all the inflow points > 1000 ml/hr could be explained by the geologically most probable conductors. The initial interpretation is that this is not a successful system for finding conductive fractures. However, it is recognised that fractures that are observed as being conductive may be connected to a geological structure of significance and not necessarily being the major structure. This interpretation assumes that the geological structures work as the major conductors even if the actual intersected conductors may be splays or other fractures related to the main geological features, c.f. **Figure 2-5**. However, mapping

only the conductive fracture geometry will not reveal the system of conductors that governs transport over larger distances. Hermanson and Tullborg (in prep) use the geology in the True Block Scale volume to explain the larger pattern that governs flow and transport in this part of the laboratory.

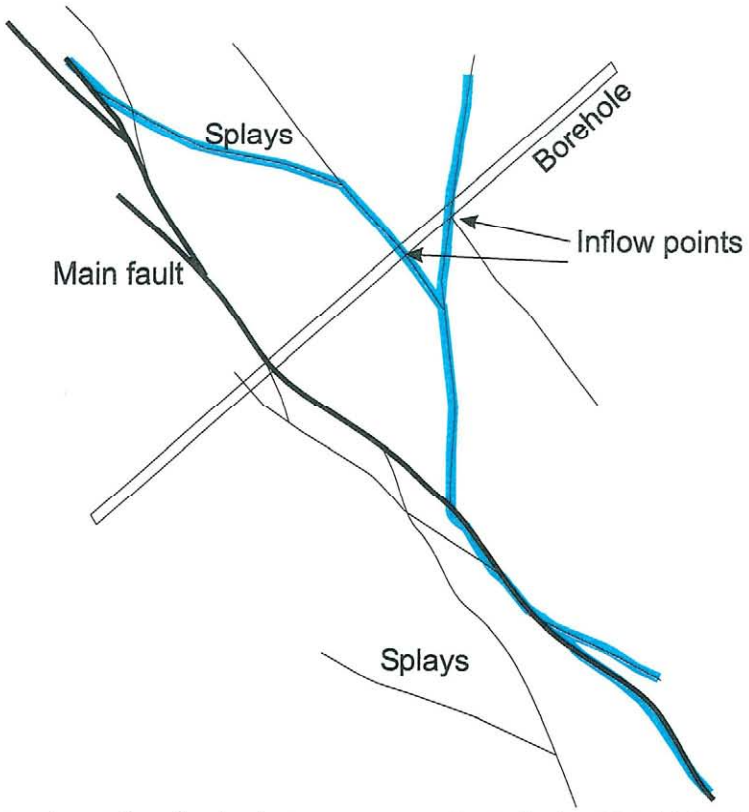

Figure 2-5 *Illustration of geological structures such as faults (thick black line) and splay fractures (thin black lines) and how the water (blue line) follows the main structure but not necessarily along the main fault plane. This effect implies that single inflow points along a borehole may give a distorted picture of what structure governs flow in the volume.*

3 March 2000 Structural model

The conceptualisation of the structural model is constrained by what is considered to be flowing or conductive structures. There is a wide choice of possible geological features in each borehole that has been delimited by either detailed hydraulic logs coupled to fractures or by geological indications if no other information is available. The tracer tests in TRUE Block Scale are to be performed in conductive pathways, which may or may not follow the major geological features in the model. The structural model aims at reflecting these conductive pathways, although this may not reflect how each geological structure extend nor the different geology along the conductive pathway. The hypothesis illustrated in **Figure 2-5** emphasises the fact that water flows through portions of large faults but also along splay fractures connected to other fractures, faults or fracture zones. The structural model honours the locations of the major inflow points as observed in the boreholes as well as making an attempt to couple these inflow points through the larger geological features in the rock mass.

The structural model presents a selection of conductive features intersecting the studied rock volume outside of the larger zones. Even though the POSIVA flow log has a very good resolution it still measures inflow at discrete points in the rock mass. Experience tells us that flow occurs along pathways in the fracture system. Boreholes may miss the pathway, but may intersect a fracture without showing any observable flow. Interpreting how water flows through the fracture network is not trivial and is assessed by utilising several indicative characteristics of the fractures themselves.

A structural model attempts to connect the points of hydraulic inflow by extending the structures between boreholes. The aids for doing this extension in space are;

- orientation of fractures at the borehole intersection
- radar or seismic reflectors
- geological signature
- responses to drilling
- hydraulic tests (cross-hole interference tests)
- transport tests

With the experience from previous investigations (Hermanson 2000) we know that by geophysics and geology alone only around 2/5 of the most conductive structures will be found. In order to increase this ratio we need to make use of the hydraulics of the fractured system. Drilling responses and hydraulic tests show us how things connect and give invaluable clues how to extend the features between the boreholes. An hydraulic approach to reconciling the interpreted structures will be presented in Chapter 4.

The identification of the deterministic structures is a combination of the geological characteristics and the hydraulic behaviour.

This chapter describes the structural geological character of each structure and presents this in the context of a conceptual hydro-structural model of the largest conductors in the block. This model reflects mainly the geological character of the identified features.

3.1 Differences between the March ´00 and the March ´99 structural models

The identified conductors interpreted from the POSIVA flow log and the BIPS system is compared with information from the March ´99 structural model. The outcome of the new data set has had the following impact of the main conceptual interpretation;

- the new borehole KI0025F03 has invoked detailed information primarily in the centre of the block.
- the POSIVA flow log has with its detailed resolution slightly changed the exact location of features #6, #7, #13, #19 and #20, #21, #22 and added two new structures called #23 and #24.

The following features are not updated from the March ´99 structural model but details are again given here for completeness. Feature number and Type is given according to the terminology presented by Hermanson (1998).

1. Fracture
This structure appears as an open fracture at L=12.5 m in KA2563A. A magnitude 1U radar reflector is interpreted to intersect KA2563A at L=11.9 m. Large steep water-bearing fractures in the TBM tunnel sections around 2600 m, and in the F-tunnel coincide with a planar interpolation of this feature trending 335/82. The average width is estimated to 1 cm based on the single intercept in KA2563A.

2. Fracture-Zone
A fairly steep structure (109/89) associated with a fractured and oxidised core at L=11.1 m, and at L=12.3 m in KA3510A (large open fracture with cavities). Similar geology is found also in KA2563A at L=68.5 m. A water-bearing fault at tunnel section L=2511 m is sub-parallel to this structure. The fracturing in the core section of Ka2563A is characterised by a network of fractures with cavities and epidotized fillings. The average width of the structure is estimated to 82 cm.

3. Zone
A steep structure sub-parallel to structure #2 (110/81) intersecting KA3510A at L=37.5 m and KA2563A at L= 68.5 m. Both intercepts are characterised by severe fracturing and faulting, brecciation and core crush (zone). There are radar indications in both cores. The width varies between 40-220 cm in KA3510A and KA2563A respectively.

4. Fracture-Fault
This feature, trending 302/82, intersects KA2563A at L= 94 m and is associated with an inflow of around 40 l/min. A possible intercept of this structure is located at L=12.9 m in KA3510A. The intercept in KA2563A is characterised by oxidised and altered host rock with calcite filled fractures with cavities. A planar interpolation of structure #4 to KA2511A yields at its intercept at L= 23 m where the rock show similar geological characteristics as in KA2563A. The section 23.08-26.6 m has a recorded inflow of 30 l/min. If Structure #4 is extended to intersect KA2511A, it is interpreted to intersect Structure #5 somewhere between KA2563A and KA2511A. Hydraulic responses from both drilling records and from the performed interference tests support the interpretation that Structures #4 and #5 are hydraulically coupled. The structure seem to be fairly consistent in width in all intercepts of around 10 cm.

5. Fracture-Fault
A structure associated with large inflows in both KA3510A, KA2563A, KI0025F and KI0023B. Interpreted to intersect at L=47.7 m in KA3510A, at L=102-103 m in KA2563A, at L = 4.9 m in KI0025F and at L=7.2 m in KI0023B. The extreme inflow in KA2563A at L = 103 m (700 l/min) occurred through a fault with 0.5-1 cm calcite and possible lithified gouge filling which is partly eroded. The fault has no clearly visible ductile precursor and occurs in diorite with no signs (such as decrease in grain size or chemical dissolution of minerals) of previous tectonic events. The feature consists of a smaller fracture ending at an almost orthogonal angle to the fault and could be interpreted as a splay fracture. A fair bit of displacement has occurred along the fault plane as opposite sides match poorly.

This structure seem to consist of one or a few major inter-linked fracture planes with rather thick (mm to cm) calcite filling, occasionally with idiomorphic crystals giving the structure a high porosity. The planar orientation (113/90) is striking as the structure is identified over a distance of at least 50 m and show more or less the same orientation. The connection to KA2511A is interpreted to occur through structure 4. Hydraulic responses are observed in the innermost section of KA2512A. Geologically this section contains subparallel fracturing to both structures #5 and #4.

8. Fault-Zone
This steeply dipping structure is interpreted to intersect the TBM tunnel, the F-tunnel, KA3510A and KA2563A. However, its angle in relation to KA2563A makes it difficult to determine the exact intersection point. Steep faults in the F- tunnel and in the TBM tunnel are well traced to KA3510A from 15.5 m up to 17.4 m in highly foliated, oxidised and altered diorite. The structure is interpreted to intersect KA2563A at around L=220-250 m. The specific intercept seems to be distributed over a larger distance consisting of foliated and altered diorite with a group of faults filled with epidote and calcite. Radar reflectors are interpreted in both KA3510A and KA2563A. As the intercept is more intense in KA3510A, the structure is either diverting into several smaller fault structures or is diminishing beyond KA2563A. The average width is 50 cm although its total width in KA2563A may be in the order of several metres if it divide into smaller branches.

10. Fracture-Fault-Zone
Both radar and seismics in boreholes KA2563A, KA2511A and in KI0023B support the current interpretation of structure 10. This is a variable structure appearing as a zone in one intercept in KI0023B, single faults and fractures in KA2563A and KA2511A, respectively. The orientation of the radar reflector in KA2511A (111/85) is consistent in orientation with the crosshole seismic reflector in KA2563A (115/79). Fractured fine-grained granite dominate in KA2511A together with minor amounts of greenstone. Fracturing is more intense in the contact between the fine-grained granite and the greenstone. The intercept in KI0023B exhibits a zone-like characteristic and dominates the width of the structure which varies between less than a cm in KA2511A to 30 cm in KI0023B.

11. Fault
This structure is indicated by crosshole seismic and radar in KA2511A at L=259 m. Indications in KA2563A consist of a steep and a sub-horizontal open fault in diorite.

Current interpretation of its orientation is 288/88. The width is approximately 15 cm, but may vary as it is picked up by crosshole seismics. It has not been tested in any hydraulic test program and little is known of its connectivity.

12. Unknown type
A seismic reflector beyond the limit of all boreholes is interpreted as being a possible boundary zone as proposed by the previous block scale siting investigation. Its orientation is 355/90.

15. Fault
A radar reflector and a number of faults in KA3510A describe this structure. At 117.90-120.89 m, 15 faults intersect KA3510A in fine-grained granite. There is a cm wide sub-parallel calcite filled fracture in the middle of this group. Although it is sealed in the drill core, it may well be conductive in more porous sections outside the borehole. It seems possible that these fractures take part in the measured slow increase in inflow as registered during drilling of this borehole. Structure #15 is substantiated by hydraulic responses in the innermost sections of KA3573A and is also supported by radar reflectors in the same section. Preliminary results from hydraulic interference tests indicate that structure #15 may be in contact with several other structures, in particular structure #7 and possibly also structure #6 (Andersson et al (1998). Its orientation is interpreted to 268/88.

16. Zone (subhorizontal)
Evidence exists for a gently dipping fine-grained granite body intersecting KA2563A at L= ca 56 m. The structure is associated with greenstone, massive faulting and core crush in KA2511A at L = 104-105 m. It is also supported by an interpreted seismic crosshole reflector and the orientation of the sub-horizontal rock contacts in both KA2563A and in KA2511A. The structure can be described as a fractured lithological body with variable thickness, extent and degree of fracturing rather than a traditional zone. However Structure #16 may be an important hydraulic connector between steep NW trending zones. The orientation is estimated to 177/18 and the average width to 110 cm.

17. Fracture (subhorizontal)
This structure is also most probably a gently dipping fine-grained granite associated with greenstone in KA2563A at L=109 m, and with an intensely deformed fine-grained granite in KA2511A at L= 133 m.. The lithological body is interpreted to follow a gently dipping cross-hole seismic reflector intersecting KA2563A at L=110.5 m and KA2511A at L=125 m. Previous seismic investigations in KA2511A also show a gently dipping reflector at this depth. There are also several sub-horizontal faults in KA2511A, in section L = 130 - 132 m, associated with altered diorite and fine-grained granite, calcite and epidote fillings. This structure is geologically more prominent than Structure #16, but is not necessarily a conductive structure as the deformation (in KA2511A) is ductile and not brittle. The orientation is estimated to 245/05 and the average width to 190 cm.

18. Fracture-Swarm-Fault (subhorizontal)
The last identified gently dipping fine-grained granite structure is supported by both radar and seismics in KA2563A and KA2511A respectively. It is interpreted to be a dry intercept in KA2511A. However, the flow log resolution does not exclude that this is a

conductive feature. This structure intersects at L=242.5 m, next to the conductive structure #10 (L=240.5 m). Inspection of the core shows a fault crush with a parallel epidotized fault in KA2511A. The main fault has chlorite and some calcite fillings and occurs in fine-grained granite (close to the contact with the diorite). The host rock in this core section (25 cm) is influenced by hydrothermal activities in KA2563A it occurs at L= 109 m with a similar geological signature. This structure is also supported by a radar reflector in KA2563A at L=191 m and a seismic reflector in KA2511A at L=240 m. The width is estimated to 20 cm and the orientation is 024/16. Further, the structure is also identified as a fracture swarm in KI0023B at L=75.5 m, supported by borehole radar and seismics. However, the performed interference test program by Andersson et al (1998) show, in a test in KA2563A that there exists no connectivity in structure #18.

Z. Zone
The Z structure is a large zone, unlike all other structures found in the drilled boreholes in the TRUE Block Scale experiment as regards to its geological characteristics. This structure is identified by a large section of core crush in KI0025F from L = 188 m to the end of the borehole which is also confirmed by the BIPS image from the same borehole. During the drilling of KI0025F it was featured by successively increased inflow and mobilisation of unconsolidated material. A mineralogical analysis performed by Tullborg (1998) show that the characteristics of this zone is similar to the characteristics of Zone NE-1, with brecciated, crushed and faulted rock with large portions of altered host rock, (diorite and fine grained granite). The contents of fault gouge in the analysed sample was low, possibly due to the fact that gouge may have been flushed out during drilling and uptake of the core. Geometrically, this zone is sub-parallel to NE-2, EW-3 and NE-1. However, based on the conceptual model of the site scale zones (Rhén, 1997), zone NE-1 is located over 80 m south of the Z structure, and EW-3 is approximately 30 m south of the Z structure. However, zones NE-2, EW-3 and NE-1 are not well identified in this particular part of the HRL. Splay structures and minor branches to these major zones may therefore exist. It is interpreted that the Z structure is such a branch of either EW-3 or NE-1. The characteristics of zone NE-2 is completely different, dominated by mylonites, and a few conductive faults.

NE-2 This zone is NE-2 and data for this zone can be obtained from Rhén et al (1997). No intercepts of this zone have been identified in the TRUE Block Scale set of boreholes.

EW-1 This zone is EW-1 and data for this zone can be obtained Rhén et al (1997).

EW-3 occurs as a zone deviating westwards from NE-1. Data for this zone can be obtained from Rhén et al (1997).

3.2 New and updated interpretations

The fractures that can be correlated to the POSIVA flow log anomalies in borehole KI0025F03 are illustrated in **Figure 3-1**. A systematic control of interpreted intercepts in the March'99 structural model showed that with the POSIVA flow log it was possible to identify the specific conductive fracture among many possible fractures in a borehole section. Table 3-1 shows the data for old (unchanged) and new intercepts interpreted to

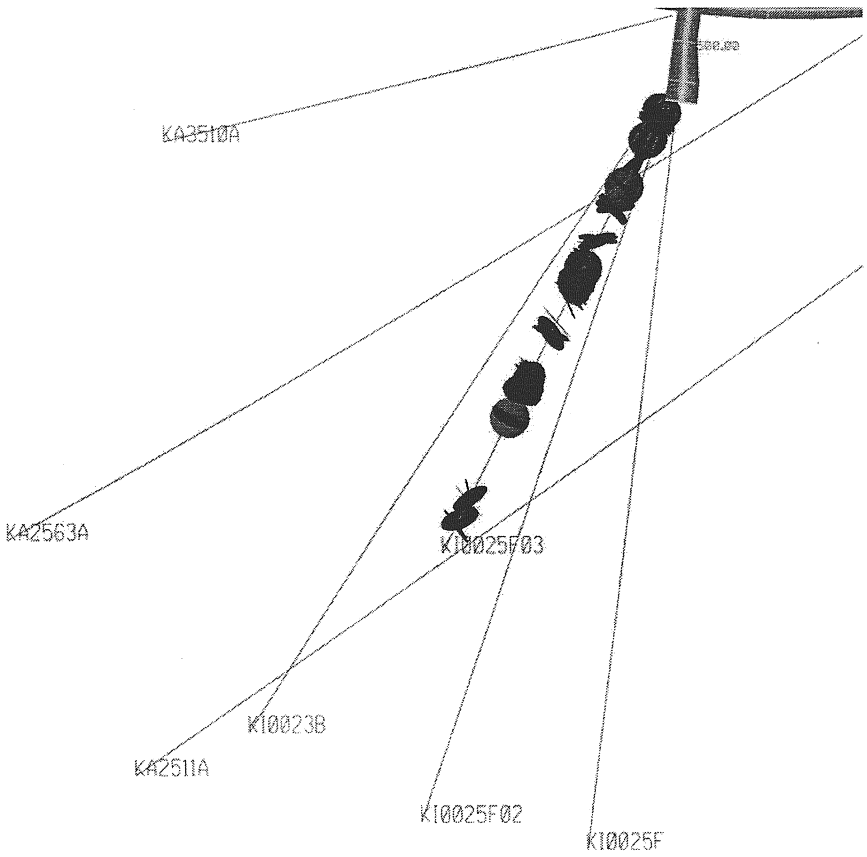

Figure 3-1. *Illustration of the fractures that can be correlated to sections of high inflow in borehole KI0025F03.*

be part of the identified conductive structures. The new information do in most cases induce minute changes of the orientation of the structures. However, two new conductors, #23 and #24, has been identified.

The geological signature of identified intercepts of structures #6, #7, #13, #19, #20, #21, #22, #23 and #24 are shown in Appendix B as extracted BIPS images and the location and orientation is given in Table 3-1 and in the March´00 structural model in **Figure 3-2**. The updated structures are all more or less steeply dipping. Below follows a condensed summary of the geological character of each updated structure:

6. Fault-Fracture
Structure #6 is observed in boreholes KI0025F03, Ki0025F02, KI0025F, KA2511A, KA2563A and KI0023B, c.f. Table 3-1 and Appendix B. These intercept points correlate well with observed points of inflow in these boreholes. However, the geological signature is not simple throughout all intercepts which either suggests a variable geology along the structure or, more likely that flow goes through more than one fracture connected in a more or less systematic way. The geology is similar in KI0025F, KI0025F02, KI0025F03 and in KI0023B which exhibits one dominant fault filled partly with calcite. The complete ductile structure has a width, which varies between 5 to 10 cm. The brittle part is constrained to one or two fault planes along the

edge of the structure. KA2511 and KA2563 show one or two weaker fractures intersecting undeformed dioritic host rock.

7. Fault
Structure #7 is heterogeneous and possibly consists of more than one fracture. This structure intersects KI0025F, F02, F03, KI0023B, KA2563 and KA2511A. The geological signature varies from a 15 cm wide brittle fault in KI0025F02, -F03 and KA2563A to a less pronounced fracture in more or less undeformed diorite in the other boreholes, c.f. Appendix B. The plastic deformation in KI0025F02 and -F03 is intense with a single fault plane and associated splay fractures.

13. Fault
Structure #13 is well pronounced in boreholes KI0025F02, -F03, KI0023B and KA2563A. This is a major fault with a maximum width of 25 cm altered host rock with mylonite in the central part. The brittle reactivation is located in the centre of the fault. The diorite around the fault is unusually black and exhibits a porphyry character of feldspars in a black matrix. Some of the intercepts show that this structure may be correlated to the contact between fine grained granite, greenstone and diorite. This is considered to be a single feature although several of the other structures are hydraulically connected to this feature.

19. Fault
Structure #19 is the most persistent structure identified so far. The extent of this structure spans over all boreholes over a distance of more than 300 m. It is identified in boreholes KA2511A, KA2563A, KI0023B, KI0025F, -F02 and -F03. The geological signature is fairly consistent throughout all boreholes and shows a 10 to 40 cm wide fault with more or less ductile and brittle deformation. The ductile deformation and alteration varies from being located around a single fault plane (KI0025F02, F03 and KI0023B) to a more fractured reddish altered structure (KI0025F, KA2511A and KA2563A). This structure is remarkably planar throughout the volume.

20. Fault-fracture
Structure #20 is observed in boreholes KI0025F, F02, F03, KA2511A, KA2563A and KI0023B. The geological signature is complex and suggests that this structure either dies out or splays off in KA2511A and KI0025F as these intercepts show little fracturing in slightly altered diorite. The other intercepts exhibit the same type of fault as found in structure #13 with a fractured core of a 10 to 15 cm wide mylonite.The core of the structure most commonly exhibits a double fault plane with mm wide calcite fillings.

21. Fracture
Structure #21 is observed in boreholes KI0023B, KI0025F and KI0025F02. The structure consists of several closely spaced fractures that have mineral fillings of calcite and chlorite. The structure cuts through altered diorite or fine-grained granite. However, the character is varied as well as the individual orientations of the intercepts which suggests that this is a complex structure of two or more splays to a larger geological structure.

22. Fault-fracture

Structure #22 is subparallel to #21 and is, in most intercepts, a fault with several subparallel fault planes. Crush is observed in the core of KI0025F03. It is also observed in boreholes KI0025F and KI0025F02 only. However, the intercept in KI0025F is a small fracture cutting through altered diorite whereas the other intercepts are 15 cm wide faults with a mylonitic core. The host rock is dark diorite with an almost porphyry character.

23. Fracture

Structure #23 is a newly identified structure based on inflow points and interference tests along two boreholes, KI0025F02 and KI0025F03. The geological character of these intercepts is similar to many fractures along the boreholes and is characterised by single fracture planes in altered dioritic host rock. The orientation is consistent in both intercepts.

Figure 3-2 illustrates the complete updated March 1999 structural model. Table 3-1 shows a summary of all interpreted intercepts of the March 1999 structural model.

Table 3-1. Intercepts of identified structures. Red text shows new intercepts and black text shows the unchanged March´99 structural model data.

	KA2563A			KA2511A			KA3510A			KI0025F			KI0023B			KI0025F02			KI0025F03		
#	Depth	Strike	Dip	Depth	Strike	Dip	Depth	Strike	Dip	Depth	Strike	Dip	Depth	Strike	Dip	Depth	Strike	Dip	Depth	Strike	Dip
1	12.5	335	82																		
2	68.5	135	87				11.1	309	75												
3	68.5	135	87				37.5	106	81												
4	94.4	296	74	23.1	300	80	12.9	115	89												
5	103.0	114	89				47.7	138	75	4.9	307	57	7.2	112	87						
6	157.2	309	89	100.1	340	71				(61.8)	342	86	44.2	88	83	52.3	317	89	51.9	136	81
7	153.4	111	73	38	143	87				43.5	253	84	42.2	103	87	39.9	126	70	43.0	88	84
8	242.4	26	84				16.1	232	89												
9	230.0	123	88																		
10	351.3	124	80	240.5	127	85							170.7	298	83						
11				258.2	288	88															
12																					
13	207.0	321	86										85.6	318	89	93.9	140	83	87.9	338	87
15							118.0	269	88												
16	56.3	11	40	104.7	233	18															
17	108.9	222	34	132.4	270	16															
18	194.3	12	18	242.5	155	9							75.5	348	41						
19	237.9	343	76	198.2	324	87				166.4	336	84	111.6	342	87	133.0	334	87	124.7	339	86
20	188.7	316	82	122	321	73				87.7	336	77	69.8	157	82	74.7	134	89	73.2	326	64
21										(166.4)	338	74	71.1	123	86	97.9	354	77	91.9	296	59
22										88.8	340	81				66.8	337	88	63.2	154	87
23																59.2	125	80	56.8	301	77
24										37.1	301	82	31.8	308	76	33.9	307	72	33.8	135	75
Z										192.1	243	77									

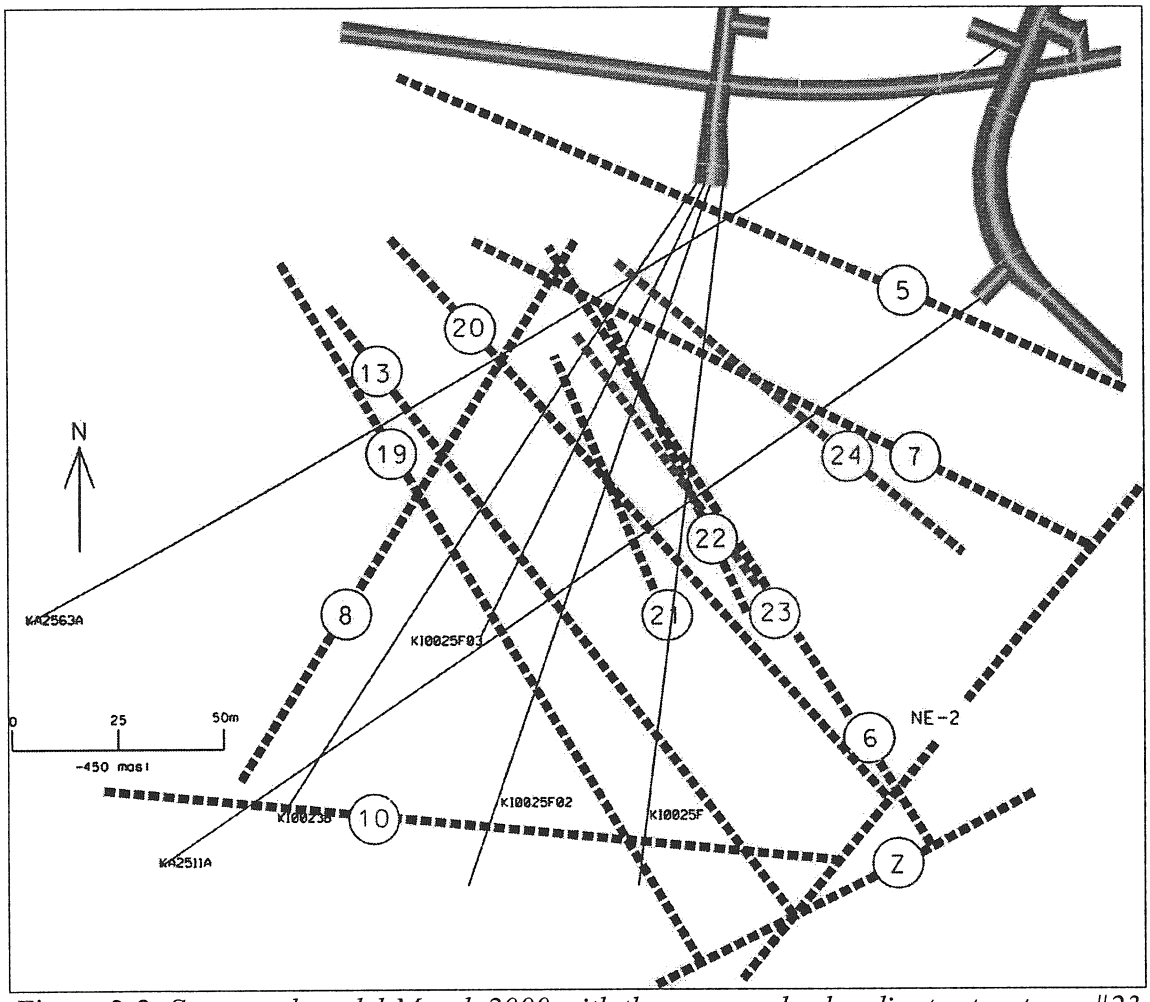

Figure 3-2. *Structural model March 2000 with the proposed subordinate structures #23 and #24.*

4 Reconciliation of the structural model and hydraulic data

Not all geologic structures are hydraulically significant. This chapter discusses how the hydraulically significant structures can be identified, and it provides data on the location and extent of these structures. This report is an update of Doe (1999) to include data from KI0025F03, which was drilled in August, 1999.

Doe (1999) presented a reconciliation of the hydraulic and structural geologic information on the TRUE Block Scale volume. The study pointed out that a subset of the September 1998 geologic structures, #6, #7, #10, #13, #19, #20, were hydraulically significant in the central part of the block. The study also described the hydraulic evidence for structures #21 and #22 that could connect the sub-parallel structures #13 and #20. The reconciliation report also proposed an additional structure, #23, that lay between Structures #22 and #6.

4.1 Pressure responses to drilling

The main sources of hydraulic data are the Posiva flow logs (Rouhiainen and Heikkinen, 1999), hydraulic tests (Gentzschein and Ludwigson, 2000), and the pressure responses to drilling, which are presented in this report. The main criteria for identifying a hydraulically significant structure are the following:

- Indications of increased outflow during drilling ,
- Pressure responses in other boreholes when the structure is penetrated by drilling,
- Locations of inflow points identified by flow logging, and
- Pressure responses across multiple boreholes during hydraulic tests

Pressure monitoring during drilling provides a very effective tool for identifying hydraulic connections. Such data were important for preparing earlier versions of the hydro-structural model. When a drill from an underground-collared hole penetrates a conducting feature it creates a sink that reduces the pressure in that conductor and other connected conducting features. If the conductor is reasonably transmissive, this pressure response can propagate rapidly through the conducting network.

Within the TRUE Block Scale volume, these pressure responses appear as sharp pressure reductions. The reductions occur very quickly, that is, within the time increments of the pressure monitoring system. As an example, Figure 4-1 shows KI0025F02's pressure responses as a function of time for the drilling of KI0025F03. The figure includes the drilling progress versus time. The light grey vertical lines show the drilling times that correspond to depths where the structural model would predict the intersection of major structures.

The pressure-time plot for KI0025F03 indicates an intersection with every major hydraulic structure in the TRUE Block Scale volume except for Structure #10, which the structural model places about 20 meters beyond the end of the hole.

Table 4-1 presents the pressure responses to drilling for each structure intersected and each monitoring interval. These pressure responses form a matrix that shows the connectivity of the structures. The responses suggest that some degree of connection exists between all the structures, but there is particularly good connection among Structures #6, #23, #22, #20, #21, and #13. We will refer to this as the Structure #20 network, as Structure #20 is the dominant and most extensive feature in the group. Although each of these structures accounts for distinct pressure responses, each intersection with one member of the network causes some response throughout the other members of the Structure #20 network.

Based on the response matrix of Table 4-1, we can conclude that the drilling of KI0025F03 confirms the basic hydraulic-structural model of the 1999 reconciliation report. The able also provides some further information on two issues identified in Doe (1999), specifically, the continuity of Structure #13 and the existence of an additional structure between #6 and #22. In addition, the analyses of drilling responses to KI0025F03 suggest an additional structure, which we refer to as Structure #24, which may lie shallow of Structure #6 and #7 but deeper than Structure #5. These clarifications are described below.

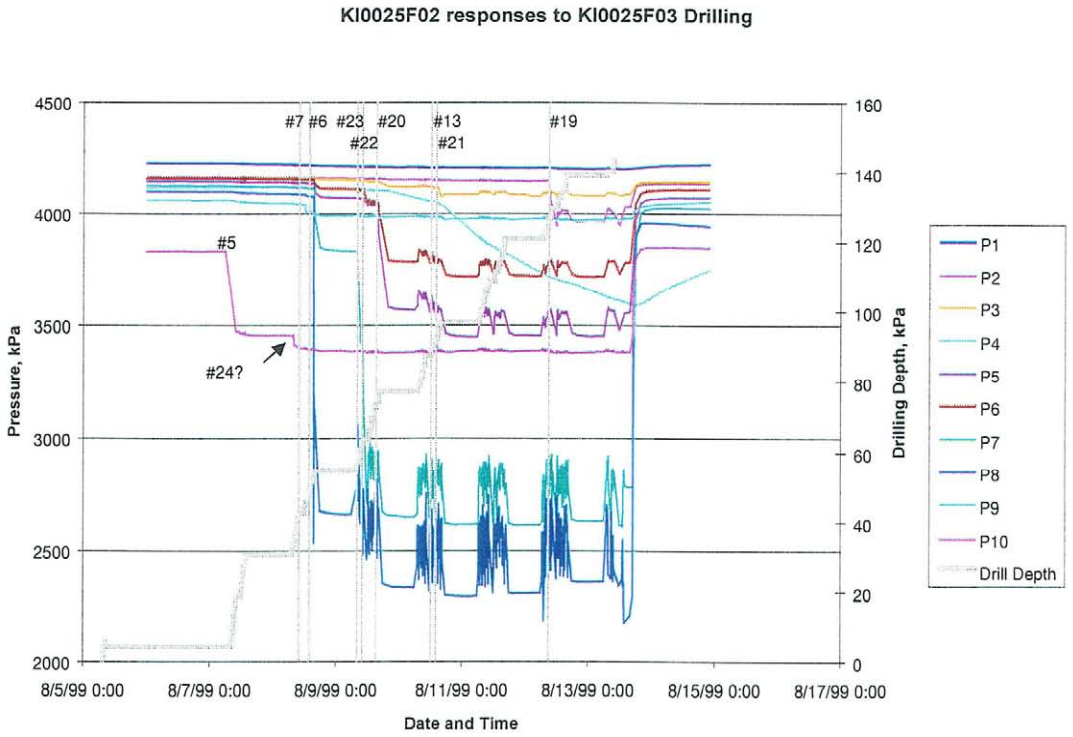

Figure 4-1. *Pressure responses of KI0025F02 to drilling in KI0025F03.*

Table 4-1. Pressure responses to drilling KI0025F03

Monitoring Intervals	Expected Structure	Pressure Responses (kPa) by Structure in KI0025F03									
		#5	#24?	#7	#6	#23	#22	#20	#13	#21	#19
KA2563:S1	#19	-	-	-	-	-	-	12	-	-	140
KA2563:S2	#19	-	-	-	-	-	-	12	-	-	143
KA2563:S3	#13	-	-	-	54	3	19	305	118	122	-
KA2563:S4	#20	-	-	-	69	5	23	416	116		-
KA2563:S5	#6,7,21	5	-	7	58	9	15	60	6	46	-
KI0023B:P1	#10	-	-	-	-	-	-	-	-	-	4
KI0023B:P2	#19	-	-	-	-	-	-	-	-	-	182
KI0023B:P3	-	-	-	-	33	-	23	226	57	130	-
KI0023B:P4	#13	-	-	-	58	6	15	320	144	145	-
KI0023B:P5	-	-	-	-	68	4	21	413	137		-
KI0023B:P6	#21	-	-	-	65	4	21	424	123		-
KI0023B:P7	#6,20	-	-	-	102	8	24	398	112		-
KI0023B:P8	#7	14	-	15	10	-	-	-	-	-	-
KI0023B:P9	#5	261	37	-	-	-	-	-	-	-	-
KI0025F02:P1	#10	-	-	-	-	-	-	-	-	-	-
KI0025F02:P2	#19	-	-	-	-	-	-	-	-	-	180
KI0025F02:P3	#13, 21	-	-	-	-	-	-	24	36		-
KI0025F02:P4	-	-	-	-	-	-	-	-	-	-	-
KI0025F02:P5	#20	-	-	-	69	4	27	470	85		-
KI0025F02:P6	#22	-	-	-	42	7	53	263	66		-
KI0025F02:P7	#23	-	-	12	280	1125	-	61	33		-
KI0025F02:P8	#6	-	-	12	1411	-	-	327	38		-
KI0025F02:P9	#7	-	-	50	-	-	-	-	-	-	-
KI0025F02:P10	#5	377	70	-	-	-	-	-	-	-	-
KI0025F:S1	Z	-	-	-	-	-	-	-	-	-	13
KI0025F:S2	#19	-	-	-	-	-	-	-	-	-	23
KI0025F:S3	-	-	-	-	-	-	-	-	-	-	23
KI0025F:S4	#20,22	-	-	-	53	3	13	396	124		-
KI0025F:S5	#6	14	7	34	10	-	-	6	10		-
KI0025F:S6	#5	186	263	-	-	-	-	-	-	-	-

There are several points worth noting in Table 4-1. The most important is the ambiguity in distinguishing Structures #21 from #13. One goal of KI0025F03 was to get a better definition of these two structures in a hole where they were clearly separated from other structures and from one another. Unfortunately, the pressure data are very noisy in the time period when these structures are intersected. This noise seems to occur mainly during periods of drilling, hence, when drilling ceases one can see clearly the pressure drops across the monitoring array that are associated with Structures #13 and #21. In most holes Table 4-1 shows the total pressure changes across both structures. With some imagination one might see a separation of the two pressure responses, and these cases are noted by giving separate pressure responses for Structures #13 and #21.

Based on the pressure responses and on the locations of conductors in the boreholes, Table 4-2 provides a matrix of which features appear in which boreholes. There is some ambiguity in this matrix for structures that are part of the Structure #20 network. Because Structure #20 intersects all boreholes except for KA2511A, every borehole has some pressure response to every structure that is part of the Structure #20 network.

This ambiguity applies to the interpretation of Structure #6 in KI0025F. There is no significant transmissivity in KI0025F in the area where Structure #6 should intersect. However, there are good pressure responses to #6 in KI0025F:S4 (which is the Structure #20 intercept), and KI0025F:P5 (which contains Structure #7 and the location where #6 should be). The possibility that the lack of a flowing point for Structure #6 is further made ambiguous by the possibility that the structure is present but does not flow locally due to channelling. Because KI0025:P5 has a Structure #6 response, and little or no Structure #20 response, the matrix of borehole intersections includes KI0025F and Structure 6 as a match but with a question mark. Other intersections that are similarly ambiguous are noted with question marks.

The matrix of structures and boreholes is very important for determining the truncations and corner locations of structures as discussed in the following section. Using this information we have prepared a structure map at Elevation = -477 masl in Figure 4-2. This map terminates structures according to which boreholes they intersect or do not intersect.

Table 4-2 Summary of structure intersections with boreholes

Structure	KI0025F	KI0025F03	KI0025F02	KI0023B	KA2563A
#5	x	x	x	x	x
#24	x	x	x	x	
#7	x	x	x	x	
#6	?	x	x	x	x
#23		x	x		
#22	x	x	x		
#20	x	x	x	x	x
#13		?	?	x	x
#21		x	x	x	?
#19	x	x	x	x	x
#10			x	x	

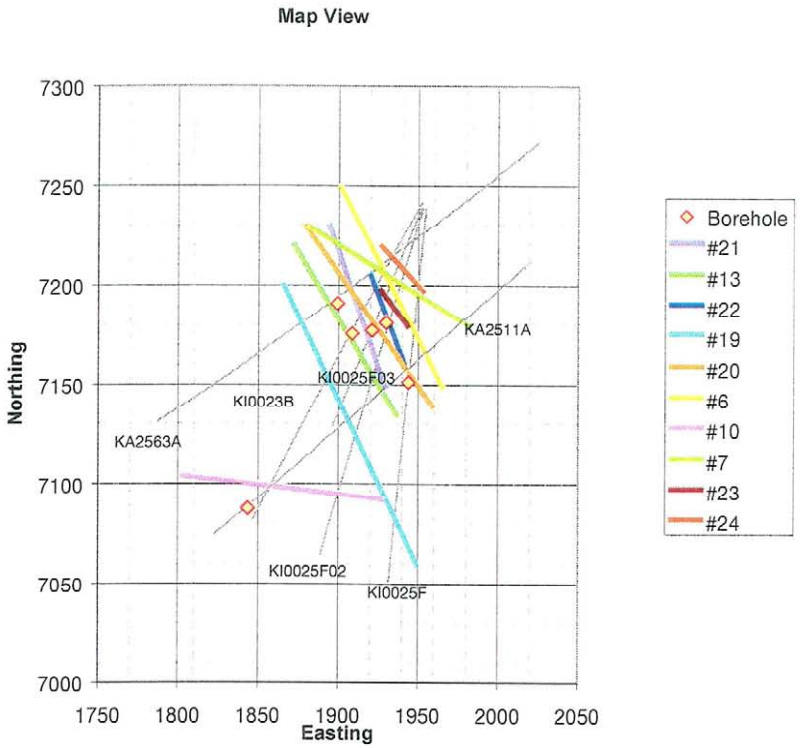

Figure 4-2. *Map of Hydraulically Significant Structures are Elevation =-477 masl.*

4.2 Further definition of Structure #13

The continuity of Structure #13 has been a source of some ambiguity since the drilling of KI0025F02 and KI0025F03. The ambiguity arose in with respect to low pressure responses of KI0025F02:P3, which should contain Structure #13, to sinks in other parts of the structure (Doe, 1999). Likewise, Structure #13 behaves similarly in KI0025F03. The two monitoring intervals, KI0025F02:P3 and KI0025F02:P3 do not respond to pumping as strongly to pumping in Structure #20 and Structure #13. This attenuated pressure response of the zones that should contain Structure #13 was shared by both KI0025F02:P3 and KI0025F03:P3 as shown by the Phase A interference tests (Andersson, and others, 2000). By contrast, KI0025F03:P3 and KI0025F02:P3 are well connected to one another as shown by the drilling responses between the two holes. Figure 4-1 shows the response of KI0025F02:P3's response to drilling of KI0025F03.

There are at least two possible explanations for the low responsiveness of the apparent Structure #13 intercepts in KI0025F02 and KI0025F03. The low responsiveness may suggest that Structure #13 is discontinuous or that the KI0025F02 and KI0025F03 intercepts represent a different structure. The possibility of non-connectivity, however,

is at odds with observations of tracer dilution responses in these intervals to pumping in other parts of the #20-#13 network.

A second explanation involves some other water source that acts as a reservoir. Such as a reservoir of water near these two intercepts can act as a constant-pressure boundary that reduces the pressure response to pumping of more distant sources. The burden for testing this hypothesis lies in identifying such a reservoir.

The possible candidate for a reservoir that can act as a constant-pressure boundary is the fracture intersection zone (FIZ) of Structures #13 and #21. Appendix C contains in-plane maps of each structure. The #13-#21 intersection can be seen in Figures C-9 and C-10. This fracture intersection zone (FIZ) passes very close to these intersections of intersections of Structure #13 in KI0025F02 and KI0025F03.

4.3 Structure #23

The previous reconciliation report (Doe, 1999) suggested the existence of a structure between Structure #6 and Structure #22 in KI0025F02. Monitoring interval KI0025F02:P7 isolates the proposed location of this structure. At the appropriate depth, the drilling of KI0025F03 produced a strong pressure response in this monitoring interval (Figure 4-1, Table 4-1). This response confirms the existence of this structure and its continuity in KI0025F03.

Based on TV and core logs, this feature is now identified as Structure #23. The structure appears definitively in only KI0025F02 and KI0025F03. It is not defined in either KI0025F or KA2563A. Its existence in KI0023B is uncertain, but could be confirmed through Posiva flow logging if the hole is opened in the future. The character of Structure #23 is different in KI0025F03 than in KI0025F02. The former hole has three or four possible flowing features on the Posiva log, while in KI0025F02 Structure #23 appears as a clear single flowing feature.

4.4 Structure #24

An inspection of the drilling responses to KI0025F03 suggested the existence of an additional structure lying somewhat shallower than Structures #6 and #7. The main evidence is a pressure response to drilling at a depth between 33.8 and 36.8 meters in KI0025F03. A review of drilling response records from previous boreholes reveals a consistent response to this structure in all holes except KA2563A. It appears in KI0025F02 (Figure 4-1), and it is particularly strong in KI0025F (Appendix C-4).

Other evidence comes from the flow logs and the borehole television data. This structure is indicated by inflow points in boreholes KI0025F02 and KI0025F03 as shown in the POSIVA flow logs by Rouhianen and Heikkinen (1998 and 1999). The intersection points in KI0023B, KI0025F, KI0025F02 and KI0025F03 fall nearly into a single plane (+/- 10 cm) with an orientation of strike of 130° and a dip of 82°. The structure consists of an open calcite fracture with limited impact of the surrounding host rock. However, the intercept in KI0025F03, c.f. Appendix B, shows signs of alteration and plastic deformation around the structure. There exists an alternative structure in

KI0025F02 at 34.9 m, although this deviates from the generally planar fit shown by the other intercepts.

In the corner model with terminations, Structure #24 is given a relatively small size, The reason for this assignment is avoidance of Structures #6 and #7. Structure #6 in particular is connected to the Structure #20-#13 network. Were Structure #24 a part of this system, it should have created some pressure response in that network (Table 4-1). Structure #24 shares monitoring intervals with Structure #5 in most boreholes. It may be part of a common network with Structure #5, however this may be difficult to test given the connections between these structures through the boreholes.

4.5 Summary of hydro-structural model

As mentioned above, the drilling and testing data from KI0025F03 largely confirm the previous hydro-structural model presented in Doe, 1999. The major features of the model are the following:

- Structure #20 is the major central structure; it is the core of a network that includes #6, #23, #22, #13, and #21.
- Structure #19 intersects all boreholes except KA2511A. It has possible connections to the Structure #20 network either through Structure #13 or through background fractures.
- Structure #13 has unusual pressure responses in KI0025F02 and KI0025F03 that may indicate either a discontinuity in the structure or a constant-pressure boundary formed by its intersection (FIZ) with Structure #21. Structure #13 does not appear in KI0025F.
- Structure #21 is part of the Structure #20 network with intersections in KI0025F02, KI0025F03, KI0023B, and possibly KA2563A. There are still some ambiguities regarding Structure #21 as it is not sufficiently separated from other structures to have unambiguous pressure responses.
- Structures #22 and #23 are confirmed by the KI0025F03 data.
- The KI0025F03 drilling pressure responses strongly suggest an additional structure, #24, which is shallow to Structures #6 and #7. This feature does not make connections with Structures #6 and #7. It is steeply dipping and likely has little effect on the behaviour of the hydraulics in the core area of the TRUE Block Scale volume.

Figure 4-3 shows a revised schematic of the connections of the structures along with inflow data.

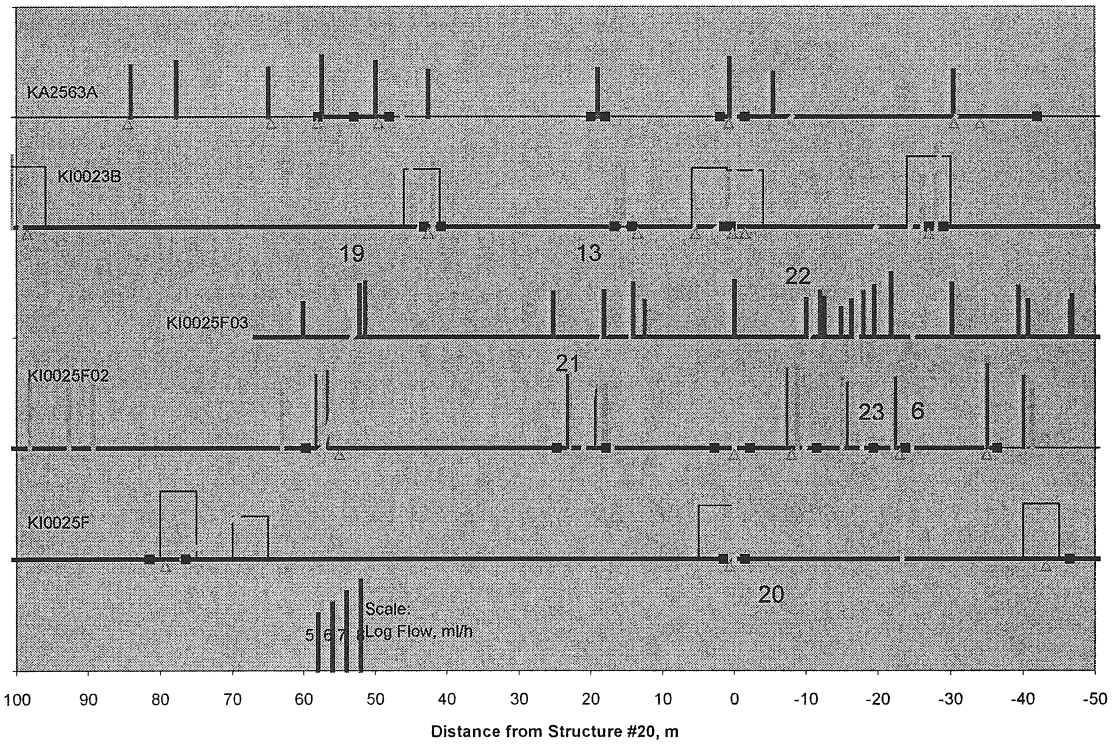

Figure 4-3. *Schematic representation of boreholes and structures with inflow data.*

4.6 Structure locations

4.6.1 Locations and feature equations

Table 4-4 provides the equations for the planes that best fit the intersections with each borehole. These equations use all holes including KI0025F03. The planes are close to those described in Doe (1999). The largest differences occur for Structures #21 and #22 which had relatively few points for the previous determinations.

Each equation describes a plane having an equation of the form $ax + by + cz + d = 0$. Some structures, particularly Structure #6, appear to have some non-planarity that accounts for discrepancies of up to a few meters in the locations on some boreholes. Adjustments for packer locations to account for planar assumptions are discussed in Section 4.6.3.

4.6.2 Corner coordinates

The corners for the features are calculated in two ways – (1) corners of structures that are extended to the edge of the 500-m TRUE Block Scale Volume, and (2) corners derived using terminations of structures based on holes not intersected by the structure.

Table 4-4 gives the corner locations assuming the structures extend to the limits of the 500-m TRUE Block Scale Volume. This approach ignores evidence that the features have limited extent.

The second method of calculating the corners (Table 4-5) uses uses information on where the structures do not appear in boreholes. This method starts by taking the trace of the structure at elevation –477 masl, which is about the centre of the main borehole array. Each trace is truncated to avoid intersections with boreholes where the structure does not appear. This truncation includes KA2511A, which limits the upward extent of the otherwise unbounded Structures #7, #6, #19, and #20.

A three-dimensional calculation of the fracture extends this trace in the dip direction of the structure by an amount equal to the trace length. This produces a square structure centered on elevation = -477 masl.

We then prepared a visualisation of the model to inspect intersections. The following adjustments were made to provide necessary connections in the network:

- Upward extension of Structure #13 to intersect Structure #19 and provide connections for Structure #19 into the other structures;
- Upward and downward extension of Structure #22 to connect over its full strike length with Structures #20 and #6;
- Upward extension of Structure #23 to provide connections with Structure #22.

4.6.3 Virtual packer locations

The structural model represents features as planes. While this is a close approximation, it is not perfect, and there can be differences of up to a few meters between the model's representation of a structure in any given borehole and its actual location. Due to these differences, the structural model may place structures at the same depths as actual packer locations. We have prepared a chart of virtual packer locations that adjusts the packer locations to be consistent with the depths in the models to avoid this cover-up problem. Most changes are minor except in KA2563 which has strong curvature. Previous versions of the virtual packer table used the collar orientation 239.48, -40.87 instead of an average over the hole of 237.59, -42.44. Table 4-6 gives the virtual packer locations for the average value.

Table 4-3. Structure plane equations

Feature Plane Equations, March '00 Model						
Structure	a	b	c	d	Strike	Dip
#6	-0.8429	-0.5374	-0.0253	-5487.00	327.5	88.6
#7	0.4404	0.8851	-0.1504	7299.84	116.5	81.4
#13	-0.7303	-0.5535	-0.4003	-5172.72	322.8	66.4
#19	-0.8586	-0.5125	-0.0126	-5285.73	329.2	89.3
#20	-0.7464	-0.6596	-0.0884	-6129.78	318.5	84.93
#21	0.8698	0.3739	-0.3221	4504.55	156.74	71.21
#22	0.8437	0.3999	-0.3580	4672.57	154.64	69.02
#23	0.7337	0.6794	0.0000	6304.34	137.2	90.0
#24	0.6391	0.7552	-0.1457	6753.70	130.24	81.62
#10	-0.0916	-0.9458	-0.3117	-6736.05	275.53	71.84

Table 4-4. Corners for structure planes extended to the TRUE block boundary.

Structure		Corners					
		1	2	3	4	5	6
#6	Easting	1784.327	1799.417	2118.921	2103.975		
	Northing	7420.639	7420.527	6919.361	6919.26		
	Elevation	-199.361	-700.79	-700.639	-199.507		
#7	Easting	1649.361	2150.793	2150.639	1649.45		
	Northing	7392.688	7143.232	7058.112	7307.397		
	Elevation	-199.361	-199.472	-700.639	-700.825		
#13	Easting	1842.699	2150.675	2150.66	1947.787	1649.385	1649.317
	Northing	7420.705	7014.25	6919.278	6919.305	7313.005	7420.613
	Elevation	-700.692	-700.551	-569.251	-199.295	-199.263	-347.88
#19	Easting	1730.108	1737.527	2036.671	2029.388		
	Northing	7420.649	7420.528	6919.351	6919.252		
	Elevation	-199.351	-700.793	-700.649	-199.502		
#20	Easting	1678.12	1737.532	2150.532	2150.665	2121.151	
	Northing	7420.609	7420.579	6953.287	6919.262	6919.338	
	Elevation	-199.481	-700.692	-700.674	-447.995	-199.461	
#21	Easting	1915.555	2130.957	1945.342	1729.951		
	Northing	7420.706	6919.275	6919.294	7420.487		
	Elevation	-199.294	-199.517	-700.706	-700.73		
#22	Easting	1936.065	2150.537	2150.52	1960.907	1723.467	
	Northing	7420.802	6968.196	6919.227	6919.378	7420.507	
	Elevation	-199.417	-199.457	-254.175	-700.782	-700.68	
#23	Easting	1720.653	1720.748	2150.533	2150.601		
	Northing	7420.575	7420.472	6956.347	6956.274		
	Elevation	-199.379	-700.765	-700.621	-199.533		
#24	Easting	1753.722	1649.372	1649.422	2150.684	2150.684	
	Northing	7420.443	7420.403	7411.863	6987.775	7084.454	
	Elevation	-199.168	-656.728	-700.739	-700.518	-199.444	

Table 4-5. Corners of structures based on terminations for non-intersections of boreholes. Local coordinates are referenced to the center of Structure #20.

Structure		Corners				Centers		DFN Input Data	
		1	2	3	4	Global	Local	Width	Length
#6	Easting	1900.12	1963.88	1902.69	1966.45	1933.28	14.07	118.60	118.63
	Northing	7249.22	7149.22	7250.78	7150.78	7200.00	-15.01		
	Elevation	-417.70	-417.70	-536.30	-536.30	-477.00	0.00		
#7	Easting	1885.40	1985.90	1877.60	1978.10	1931.75	12.53	112.25	113.55
	Northing	7237.62	7187.62	7222.43	7172.43	7205.03	-20.04		
	Elevation	-420.87	-420.87	-533.13	-533.13	-477.00	0.00		
#23	Easting	1926.76	1943.43	1926.76	1943.43	1935.09	15.88	24.53	49.06
	Northing	7198.00	7180.00	7198.00	7180.00	7189.00	-4.01		
	Elevation	-452.47	-452.47	-501.53	-501.53	-477.00	0.00		
#22	Easting	1933.48	1954.81	1903.29	1924.62	1929.05	9.83	49.80	93.34
	Northing	7211.16	7166.16	7196.85	7151.85	7181.51	3.48		
	Elevation	-439.65	-439.65	-526.80	-526.80	-483.22	-6.22		
#20	Easting	1875.46	1955.00	1883.44	1962.98	1919.22	0.00	120.11	120.58
	Northing	7226.46	7136.46	7233.52	7143.52	7184.99	0.00		
	Elevation	-416.94	-416.94	-537.06	-537.06	-477.00	0.00		
#13	Easting	1844.39	1908.82	1890.79	1955.21	1899.80	-19.41	106.66	145.49
	Northing	7198.82	7113.82	7234.04	7149.04	7173.93	11.06		
	Elevation	-397.01	-397.01	-530.33	-530.33	-463.67	13.33		
#21	Easting	1908.28	1942.67	1881.06	1915.45	1911.87	-7.35	87.08	91.98
	Northing	7235.87	7155.87	7224.18	7144.18	7190.03	-5.04		
	Elevation	-433.46	-433.46	-520.54	-520.54	-477.00	0.00		
#19	Easting	1864.97	1948.53	1866.75	1950.31	1907.64	-11.58	163.04	163.05
	Northing	7199.49	7059.49	7200.51	7060.51	7130.00	54.99		
	Elevation	-395.48	-395.48	-558.52	-558.52	-477.00	0.00		
#10	Easting	1799.34	1923.24	1807.46	1931.36	1865.35	-53.87	124.48	131.07
	Northing	7084.83	7072.83	7125.05	7113.05	7098.94	86.05		
	Elevation	-414.76	-414.76	-539.24	-539.24	-477.00	0.00		
#24	Easting	1931.11	1957.10	1923.34	1949.34	1940.22	21.00	34.06	34.93
	Northing	7220.00	7198.00	7220.00	7198.00	7209.00	-24.01		
	Elevation	-459.97	-459.97	-494.03	-494.03	-477.00	0.00		

Table 4-6. Virtual packer locations for March '00 Structural Model; blue indicates location changes from actual.

KI0025F03		KI0025F02		KI0023B		KA2563A		KI0025F		KA2511A	
P-setting		P-setting		P-setting		S-setting		S-setting		T-setting	
Collar	0	Collar	0	Collar	0	Collar	0	Collar	0	Collar	0
Pkr10	2.6	Pkr10	2.4	Pkr9	3.6	Pkr8	145	Pkr6	4	Pkr8	5
	3.58		3.4		4.6		146		5		6
#7	42.18	Pkr9	37.5	Pkr8	40.45	#7	150.85	#7	39.45	#7	36.54
Pkr9	49.00		38.5		41.45	#6	154.69	Pkr5	41.5	Pkr7	64
	50.00	#7	42.57	#7	41.81	#22?	141.69		42.5		65
#6	50.30	Pkr8	50.7	Pkr7	42.45	#21?	171.20	#6	61.81	#6?	87.50
Pkr8	54.08		51.7		43.45	Pkr7	185	Pkr4	85.5	Pkr6	95
	55.08	#6	53.32	#6	45.80		186		86.5		96
#23	56.6	Pkr7	55.1	#23?	52.65	#20	186.25	#20	86.76	Pkr5	102
Pkr7	58.58		56.1	#20	69.33	Pkr6	190	#22	88.60		103
	59.58	#23	59.2	Pkr6	69.4		191	Pkr3	89.5	Pkr4	110
#22	60.93	Pkr6	63		70.4				90.5		111
Pkr6	65.58		64	#21	70.66	Pkr5	204	#13?	109.46	#20?	120.23
	66.58	#22	67.07	Pkr5	71.95		205	Pkr2	160	#22?	129.87
#20	73.88	Pkr5	72.3		72.95	#13	205.28		161	Pkr3	138
Pkr5	74.08		73.3	Pkr4	83.75	Pkr4	208	#19	163.58		139
	75.08	#20	77.25		84.75		209	#21	167.14	#13?	148.43
		Pkr4	77.5	#13	85.79			Pkr1	169.5	#19?	153.93
Pkr4	80.00		78.5	Pkr3	86.2	Pkr3	227		170.5	#21?	156.10
	81.00	Pkr3	92.35		87.2		228	END	193.66	Pkr2	170
#21	82.07		93.35	Pkr2	110.25	#19	229.6				171
Pkr3	88.08	#13	95.07		111.25	Pkr2	241			Pkr1	238
	89.08	#21	95.90	#19	112.71		242				239
#13	90.23	Pkr2	99.25	Pkr1	112.8	Pkr1	246			#10	239.98
Pkr2	92.58		100.25		113.7		247			END	293
	93.58	#19	137.14	#10	169.45						
Pkr1	100.08	Pkr1	138	END	200.71	END	362				
	101.08		139								
#19	131.31	#10	157.20								
END	141.7	END	204.18								

4.6.4 Transmissivity data for structures

Table 4-7 updates the transmissivity data for the structures reported in Doe, 1999. The data for KI0025F03 are taken directly from Gentzschein and Ludvigson, 2000. The only modifications to these data involve summing the results of separate tests when those tests include multiple conductors that constitute a single structure. For example, Gentzschein and Ludvigson's tests 3 and 4 span Structure #23, which has multiple conductive segments. Similar summations were made for tests 5 and 6 (Structure #22) and tests 8 and 9 (Structure #13).

Table 4-7. Transmissivity data (m2/s) for March '00 Structural Model

Structure	KI0025F			KA2563A	KI0023B		KI0025F02		
	Buildup (Safir)	Buildup (Jacobs)	Pump Test	Pump Test	Buildup	Pump Test	Buildup	Flowdim	Pump Test
7	9.0E-07	1.3E-05	3.7E-05	2.1E-05	1.8E-05	4.0E-05	1.7E-06	1.8E-05	x
6	x	x	x	x	4.0E-07	x	1.5E-08	1.0E-07	x
23	x	x	x	x	x	x	5.3E-09	6.7E-09	x
22	1.8E-07	5.1E-07	8.5E-07	x	x	x	2.6E-07	3.7E-07	x
20				8.7E-07	9.6E-07	9.6E-07	6.5E-07	5.9E-07	6.90E-07
21	x	x	x	x	8.1E-07		9.6E-09	2.8E-09	x
13	x	x	x	4.5E-08	5.8E-08	3.20E-07	1.5E-09	1.7E-07	x
19	1.1E-05	2.9E-05	x	x	3.9E-06	x	1.7E-06	1.8E-07	x
10	x	x	x	x	4.5E-06	x	5.3E-08	1.2E-07	x

Structure	KI00125F		KA2563A	KI0023B		KI0025F02	
	Packer Log	Flow Test	Posiva Log	Packer Log	Flow Test	Posiva Log	Flow Test
7	6.2E-08	4.10E-07	-	-	1.6E-05	>1.6E-07	1.8E-06
6	x	x	2.2E-08	1.7E-06	3.3E-08	1.1E-08	1.5E-08
24	x	x	x	x	x	x	x
23	x	x	x	x	x	5.4E-09	1.1E-08
22	4.4E-08	1.60E-08	x	x	x	>1.0E-07	3.3E-07
20			>1.9E-07	8.9E-08	1.4E-07	>1.2E-07	1.1E-06
21	x	x	6.8E-09	1.5E-07	6.9E-07	2.8E-08	5.0E-08
13	x	x	2.7E-08	3.3E-08	9.8E-08	3.9E-09	4.6E-09
19	8.9E-07	1.40E-06	9.4E-08	1.2E-07	1.2E-06	>1.1E-7	1.1E-07
10	x	x	x	2.2E-07	2.7E-06	3.3E-08	5.3E-08

Table 3-7 Continued, Transmissivity data for March '00 structural model

KI0025F03		
Posiva Log	Flow Test	Buildup
6.30E-08	x	x
2.10E-07	1.10E-07	6.80E-08
2.98E-08	x	x
2.00E-08	1.30E-08	1.50E-08
3.50E-08	x	8.30E-09
7.50E-08	6.10E-07	6.10E-07
2.10E-08	9.60E-09	3.90E-09
6.70E-08	4.40E-08	3.80E-08
1.20E-07	x	1.30E-06
x	x	x

5 REFERENCES

Andersson, P, Ludvigsson, J-E, Wass, E., (1998). True Block Scale Project, preliminary characterization stage. Combined interference tests and tracer tests. Performance and preliminary evaluation. Äspö Hard Rock Laboratory, Technical Note TN-98-28b. Swedish Nuclear Fuel and Waste Management Company.

Adams, J., 1998. Preliminary results of selective pressure build up tests in borehole KI0023B. Technical Note TN 98-27b. Äspö Hard Rock Laboratory. Swedish Nuclear Fuel and Waste Management Company, Stockholm

Carlsten, S., 1998. Prototype repository project. Borehole radar measurements in KA3573A, KA3600F and G-boreholes. Äpö Hard Rock Laboratory progress report HRL-98-16. Swedish Nuclear Fuel and Waste Management Company, Stockholm.

Carlsten, S., 1999. True block scale project. Results from borehole radar measurements in KI0025F02. International technical document ITD-99-02. Swedish Nuclear Fuel and Waste Management Company, Stockholm.

Dahlström, L.O., 1998. Test Plan for the Prototype repository. Äspö Hard Rock Laboratory Progress Report HRL-98-24. Swedish Nuclear Fuel and Waste Management Company, Stockholm.

Gentzshein, B. and J.-E. Ludwigson, 2000, Single-hole hydraulic tests and short-term interference tests in KI0025F03, SKB Äspölaboratoriet International Technical Document ITD-00-05. Swedish Nuclear Fuel and Waste Management, Stockholm.

Hermanson, J., Follin, S., 1997, TRUE Block Scale Project. Update of the structural model using characterisation data from KA2563A, KA3510A and KA2511A. Scoping stage. SKB Äspölaboratoriet Technical Note TN-97-19b. Swedish Nuclear Fuel and Waste Management, Stockholm.

Hermanson, J. 1997, TRUE Block Scale Project. Update of the structural model using characterisation data from KA2511A and KI0025F. SKB Äspölaboratoriet Technical Note TN-97-35b. Swedish Nuclear Fuel and Waste Management, Stockholm

Hermanson, J., 1998. TRUE Block Scale Project, preliminary characterisation stage. September 1998 structural model; Update using characterisation data from KI0023B. SKB Äspölaboratoriet Technical Note TN-98-18b. Swedish Nuclear Fuel and Waste Management, Stockholm.

Munier, R., 1995. Studies of geological structures at Äspö – Comprehensive summary of results, SKB PR 25-95-21, Swedish Nuclear Fuel and Waste Management Co., Stockholm.

Patel, S., Dahlström, L.O., Stenberg, L., 1997. Characterisation of the rock mass in the Prototype repository at Äspö HRL. Stage 1. Äspö Hard Rock Laboratory Progress Report HRL-97-24. Swedish Nuclear Fuel and Waste Management Company, Stockholm.

Rhén,I, Gustafson, G., Stanfors, R., Wikberg, P. Geoscientific evaluation 1997/5, 1997. Models based on site characterisation 1986-1995 1997. SKB Technical Report, TR 97-06. Swedish Nuclear Fuel and Waste Management Company.

Rouhiainen, P., P. Heikkinen, 1999. Difference flow measurement in borehole KI0025F03 at the Äspö HRL. International Technical Document, ITD 99-26. Swedish Nuclear Fuel and Waste Management Co.

Appendix A Fractures in inflow sections in KI0025F03

djup [m]	flöde [ml/h]	strykning [°]	stupning [°]	egna kommentarer	kärnkarterarens kommentarer
0					Äspödiorit, grå medelkornig ögonförande svagt förskiffrad, α=50 °
2.4	400	298	29	tydlig	
2.4		296	34	ej synlig	
3.6	650 000	350	62	tydlig	3,50: α=50 °, calcit, Q=5,74
4.7	2 000	311	87	tydlig	4,50: α=55 °, calcit, klorit
4.7		328	84	ej synlig	
4.7		123	86	ej synlig	
5.7	35 000	299	72	5,6 bred och tydlig	
5.7		312	84	knappt synlig	
5.7		139	86	knappt synlig	
6.3	200	244	68	tydlig, matt	
6.3		329	73	omvänd sinus, ej synlig	
8.2	100	134	84	ytterkant med nedanstående	
8.2		134	84	ytterkant med ovanstående	
8.2		129	87	ej synlig	
11.6	70	071	20	synlig	10-11: 10 cm pegmatit
16.8	60	015	75	parallell med nedanstående, synlig	
16.8		015	75	parallell med ovanstående, synlig	
18.3	40	236	77	ej öppna, endast färgskiftning	
18.3		236	77	ej öppna, endast färgskiftning	
26.4	6 500	123	85	26,3 synlig spricka under	
26.4		128	86	26,3 synlig spricka under	
26.7	1 500	321	87	synlig spricka i 26,6, i övrigt flera ej synliga, se nedan	
26.7		315	79		
26.7		050	12		
26.7		050	12		
26.7		260	88		
26.7		198	14		
32.4	3 000	274 x 2	68 x 2	"dubbelspricka" synlig	32-33: röd finkornig granit
32.4		071	70		34-35: röd finkornig granit
33.8	35 000	135	75	klar öppning, ytterligare 6 sprickor under (osynliga)	36-37: röd finkornig granit
33.8		145	80	eventuellt även denna och nedanstående	
33.8		134	87		
43.0	80 000	088	84	bred spricka	
43.0		267	88	knappt synlig	
43.4	20 000	098	78	varierad sprickbredd, tydligare nedanför utan sinus, ?	
44.1	800	088	88	fem sinus, två synliga band, ?	46-47: röd finkornig granit
44.1		251	71		47-48: röd finkornig granit

djup [m]	flöde [ml/h]	strykning [°]	stupning [°]	egna kommentarer	kärnkarterarens kommentarer
51.4	250 000	147	79	osynlig	48-50: röd finkornig granit
51.4		145	80	osynlig	51-53: omvandlad diorit, mylonit ?, Qtot=11,4
51.4		132	86	osynlig	
52.0	300 000	136	81	bred	
52.9	4 000	154	17	knappt synlig, denna eller nedanstående, ?	
52.9		232	27	ej synlig	
53.8	35 000	352	82		
53.8		337	80		
55.2	10 500	147	70	klar öppning	
55.5	10 500	138	71	bredast av ytterligare tre sprickor	
56.9	2 000	300	64	lika bred som nedanstående	
56.9		301	77		
56.9		063	23	delvis bred	
57.2	200	343	83		
58.3	500	336	37	bredare än nedanstående	
58.3		330	44		
60.7	45 000	125	86	60,6 knappt synlig	
61.3	45 000	138	83	61,2 knappt synlig	
63.2	3 000	154	87	bred	63: röd finkornig granit
69.6	60	319	89	knappt synlig	
73.2	120 000	326	64	73,1 tiotal sprickor	73: Qtot=16 l/min
73.2		151	89		
73.2		291	78		
85.8	2 000	326	87		86,5-90: röd finkornig granit
87.4	75 000	137	85		
87.5	50 000	338	87	bred	
87.5		139	81	måttlig	
87.8	30 000	351	72	bred	
87.8		335	81		
87.8		039	38		
90.6	6 000	261	47	endast färgskiftning	
90.6		274	43	eventuellt även denna och nedanstående	
90.6		271	40		
91.4	20 000	301	75		
91.9	10 500	296	59		92: röd finkornig granit, Qtot=20,4 l/min
91.9		289	62		
98.5	8 000	284	84	?	96,5-98: röd finkornig granit
98.9	8 000	296	59		
99.6	90	231	7		102-103: grönsten
124.7	100 000	237	68	bred	110: Q2-slim 25 grader, 20 mm
124.7		168	87	eventuellt även denna	117-118: röd finkornig granit, Qtot=19,2 l/min
125.5	70 000	139	89	tydlig	120: grå finkornig granit
131.1	200	248	60	rött område, denna och närmaste nedan bredast	2 parallella kloritsprickor vittrade, kalcit vittrad
131.1		248	61		127,5-128,5: grönsten, Qtot=24,0
131.1		248	61		131: grönsten
133.3	1 500	144	83		132: grönsten
141.3				slut	142: Qtot=24,4, BH slut 141,72 m, Qtot=25 l/min (öppet borrhål)

Appendix B Geological signature (BIPS) of key structure intercepts

Structure #6

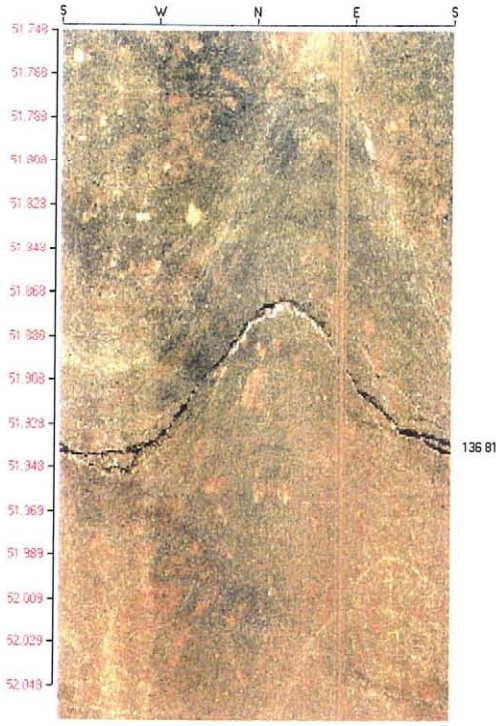

KI0025F03
L=51.9 m (136/81)

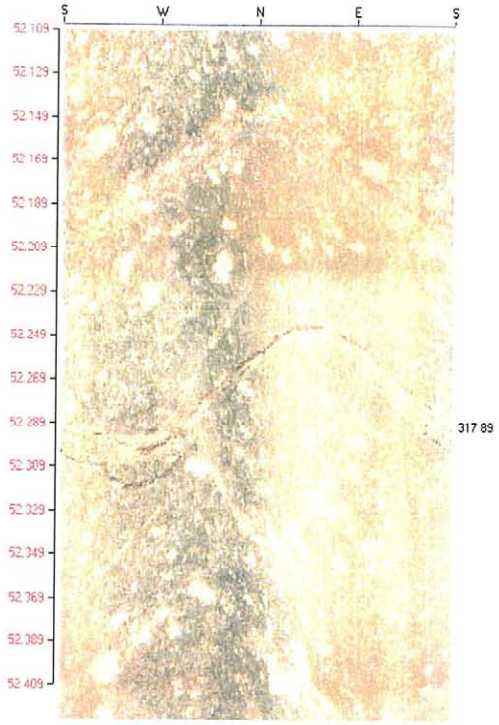

KI0025F02
L = 52.3 m (317/89)

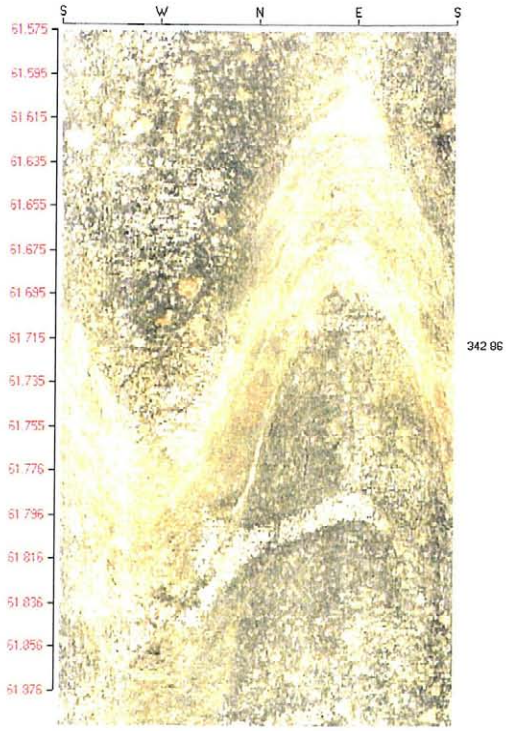

KI0025F
L = 61.8 m (342/86)

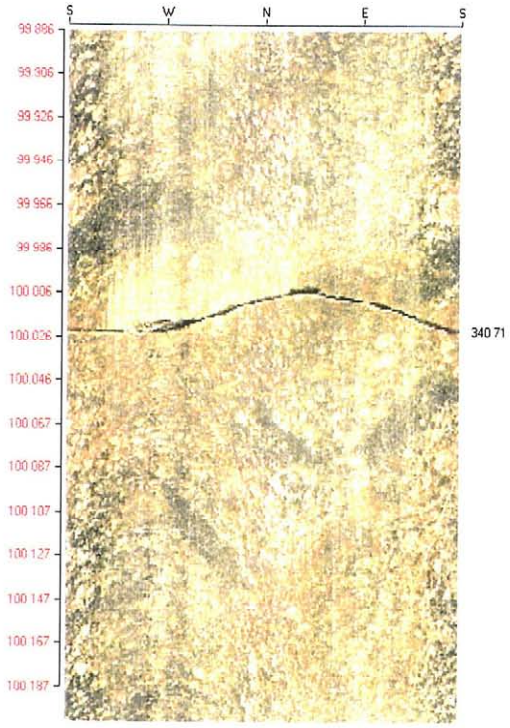

KA2511A
L = 100.1 m (340/71)

Structure #6

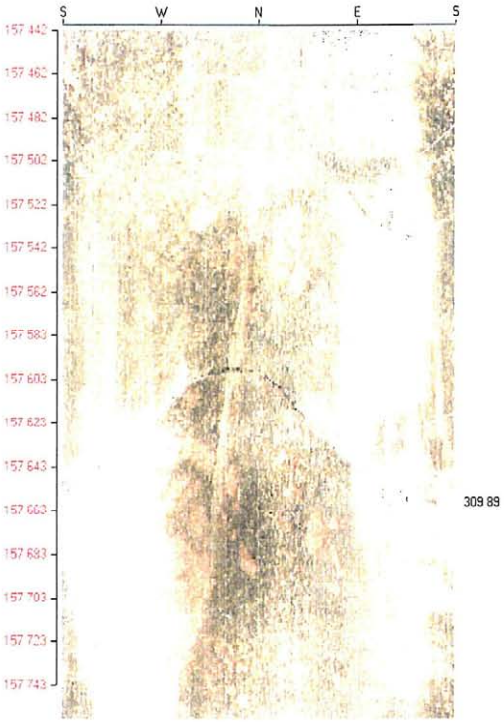

KA2563A
L = 157.2 m (309/89)

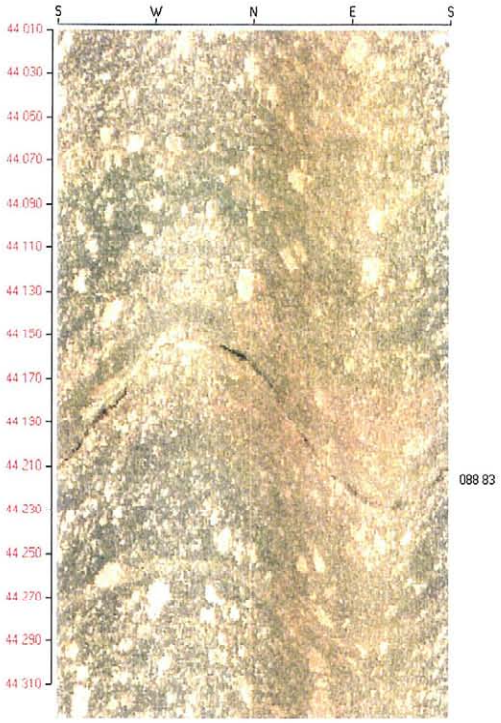

KI0023B
L = 44.2 m (88/83)

Structure #7

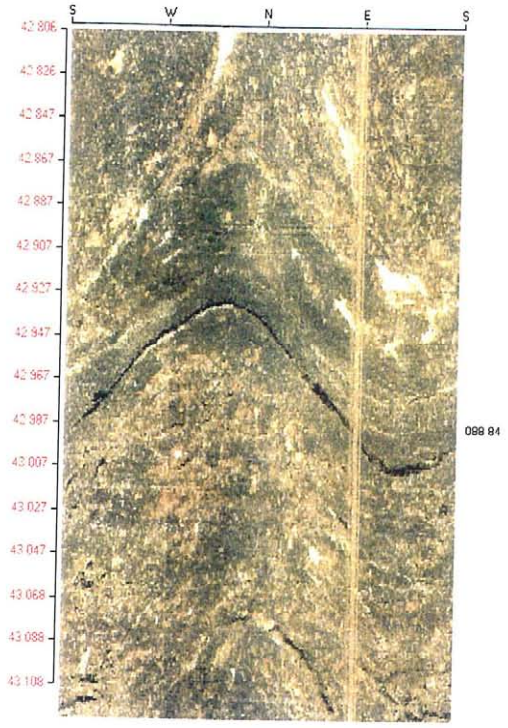

KI0025F03
L = 43.0 m (88/84)

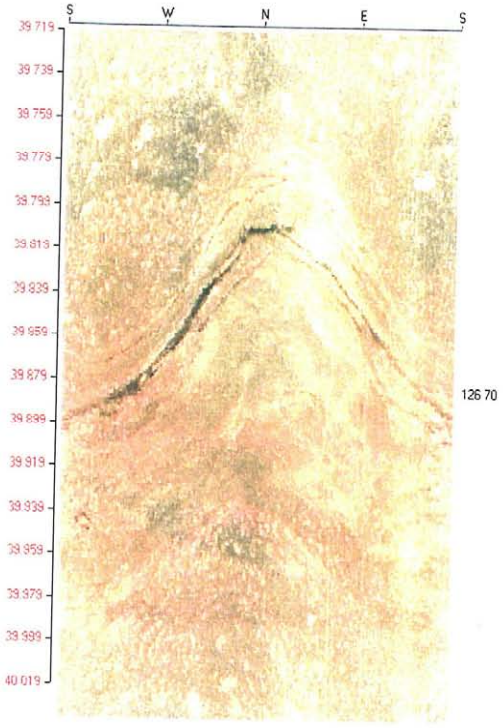

KI0025F02
L = 39.9 m (126/70)

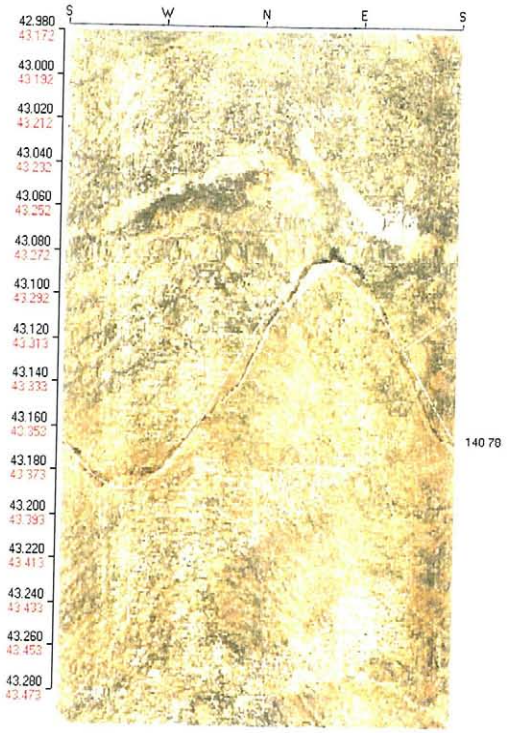

KI0025F
L = 43.2 m (140/78)

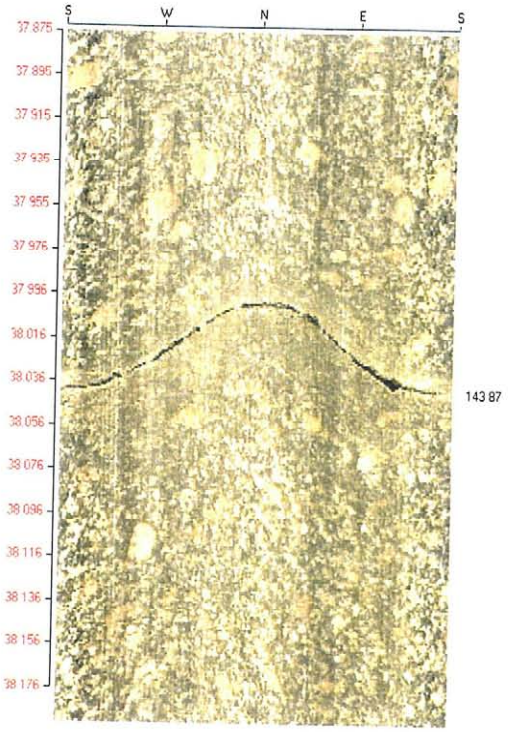

KA2511A
L = 38 m (143/87)

Structure #7

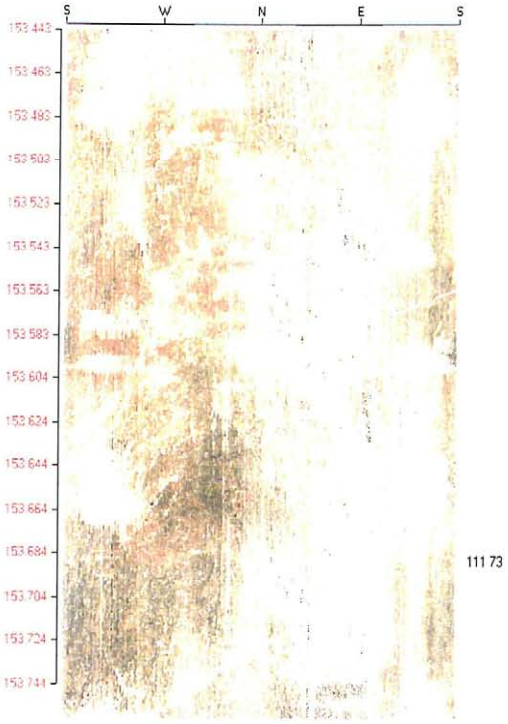

KA2563A
L = 153.4 m (111/73)

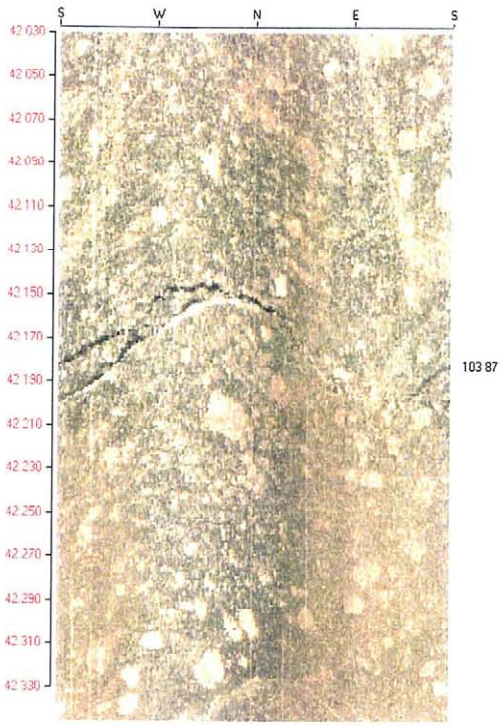

KI0023B
L = 42.2 m (103/87)

Structure #13

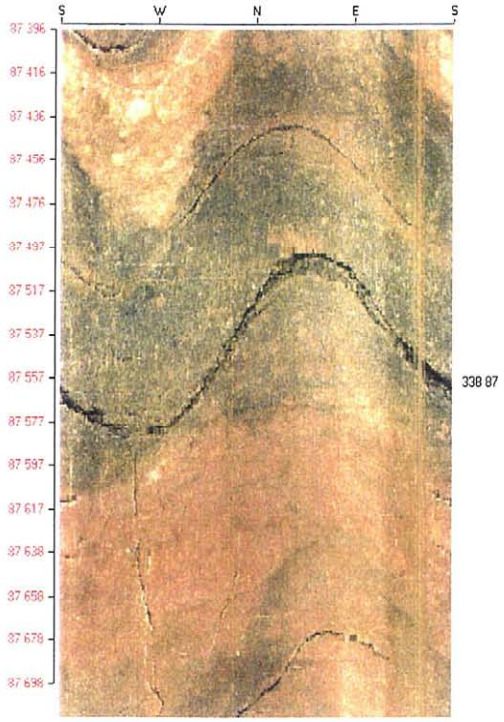

KI0025F03
L = 87.5 m (338/87)

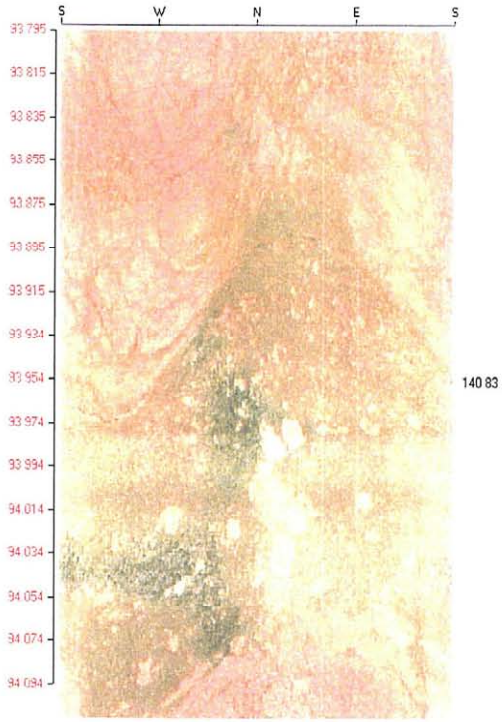

KI0025F02
L = 93.0 m (140/83)

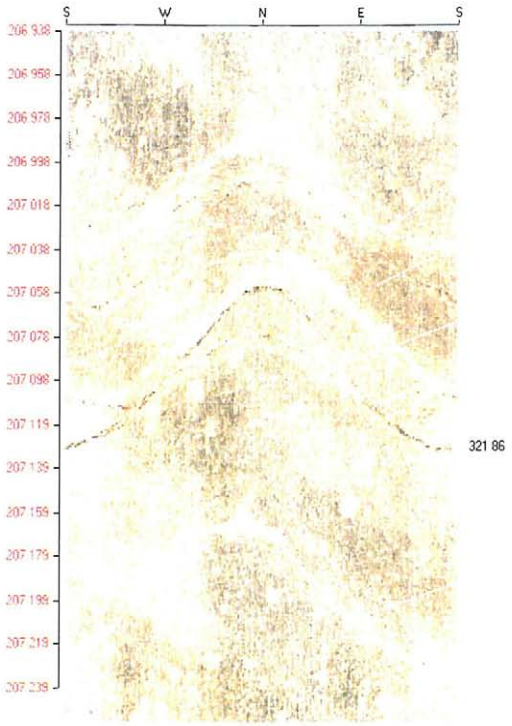

KA2563A
L = 207.0 m (321/86)

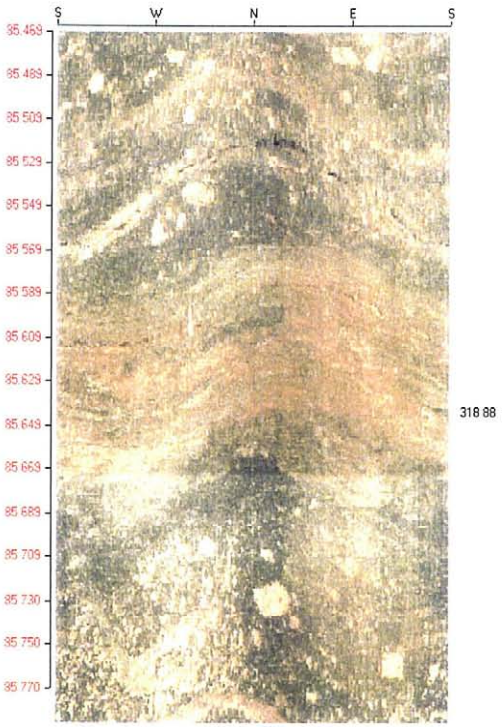

KI0023B
L = 85.6 m (318/89)

Structure #19

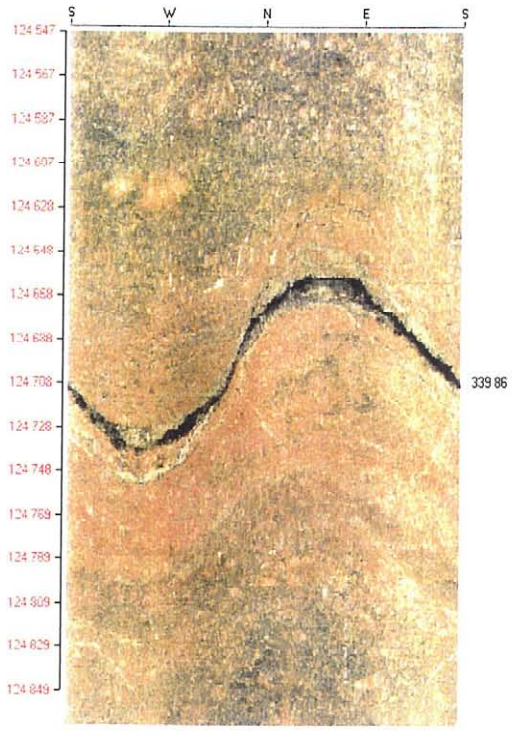

KI0025F03
L = 124.7 m (339/86)

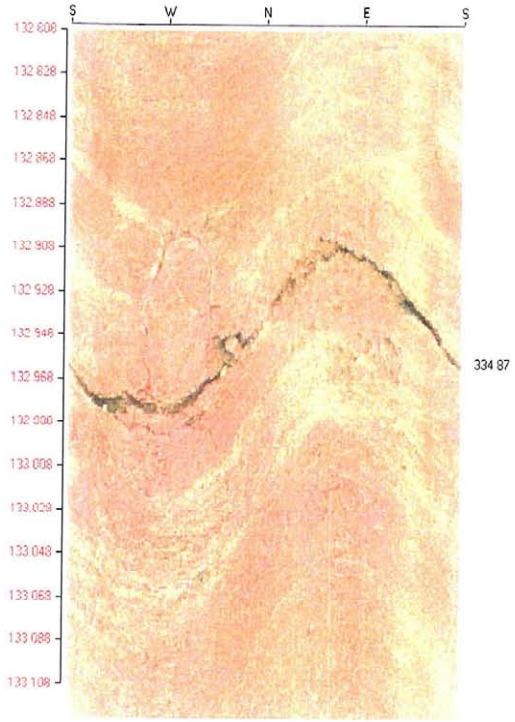

KI0025F02
L = 133.0 m (334/87)

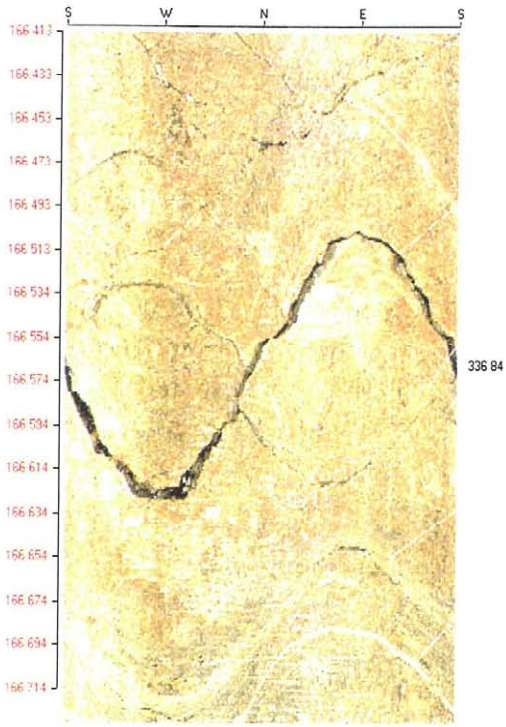

KI0025F
L = 166.4 m (336/84)

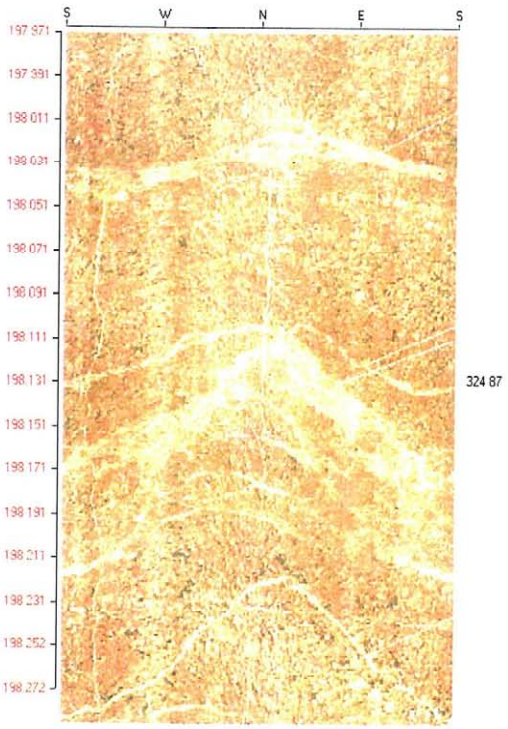

KA2511A
L = 198.2 m (324/87)

Structure #19

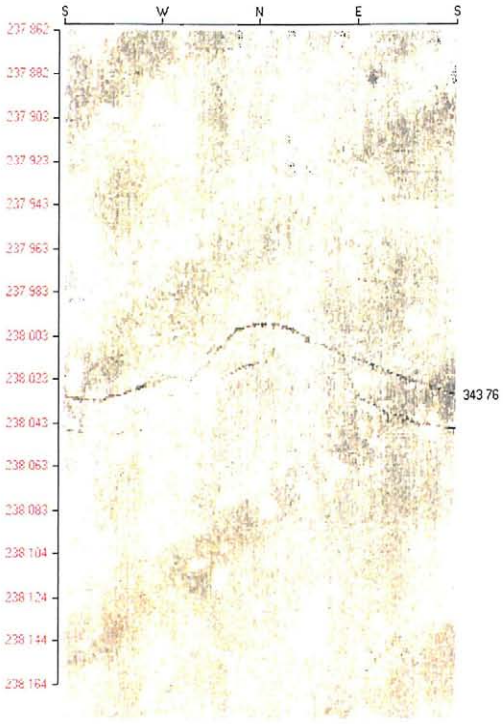

KA2563A
L = 237.9 m (343/76)

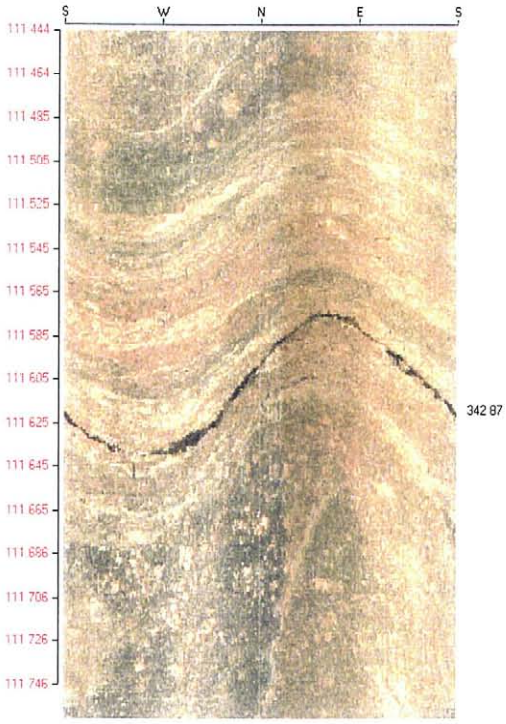

KI0023B
L = 111.6 m (342/87)

Structure #20

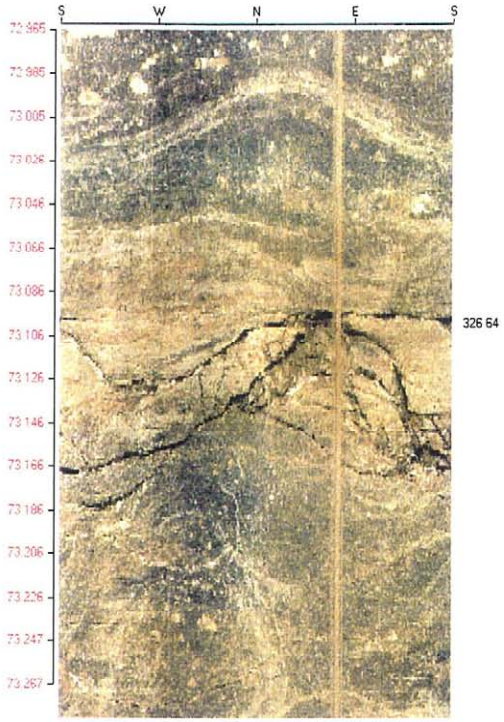

KI0025F03
L = 73.2 m (326/64)

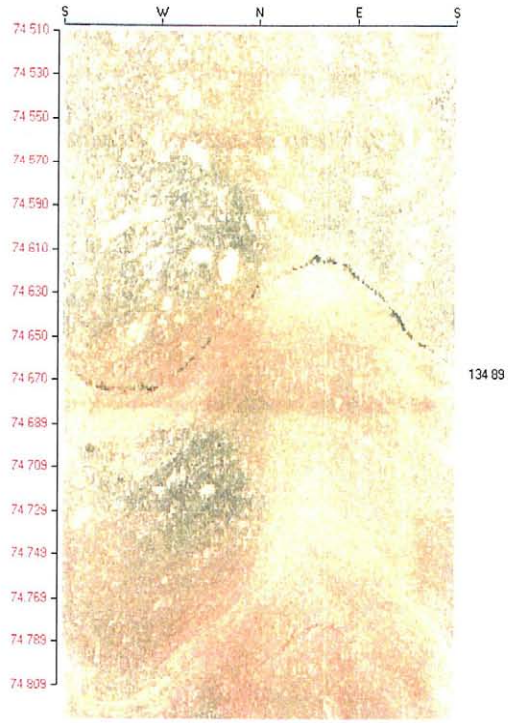

KI0025F02
L = 74.7 m (134/89)

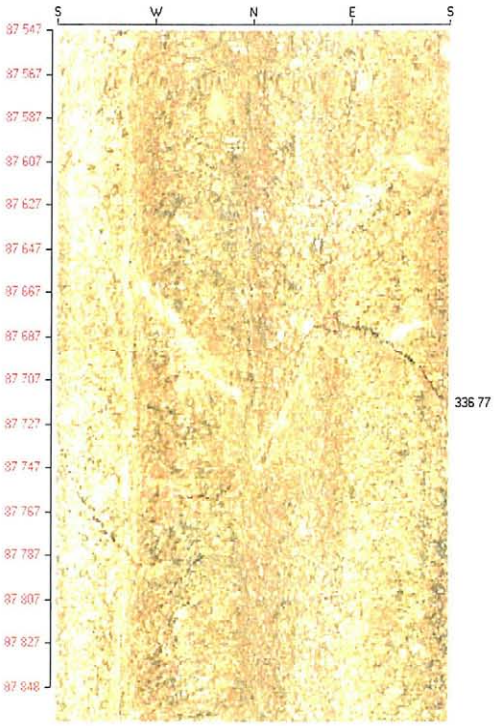

KI0025F
L = 87.7 m (336/77)

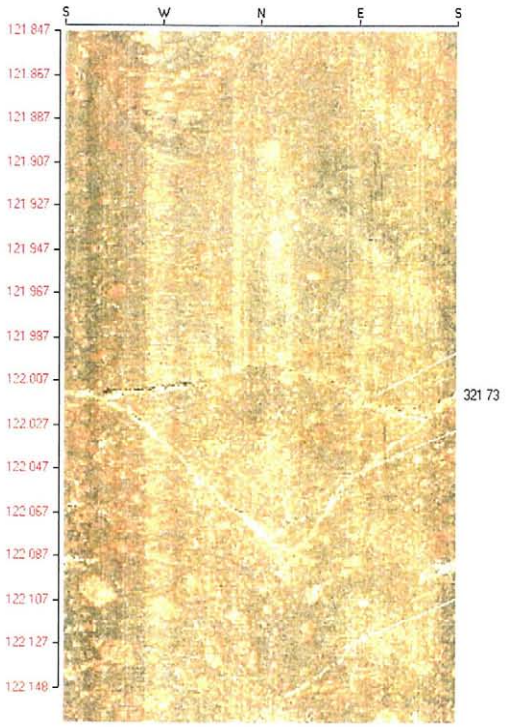

KA2511A
L = 122.0 m (321/73)

Structure #20

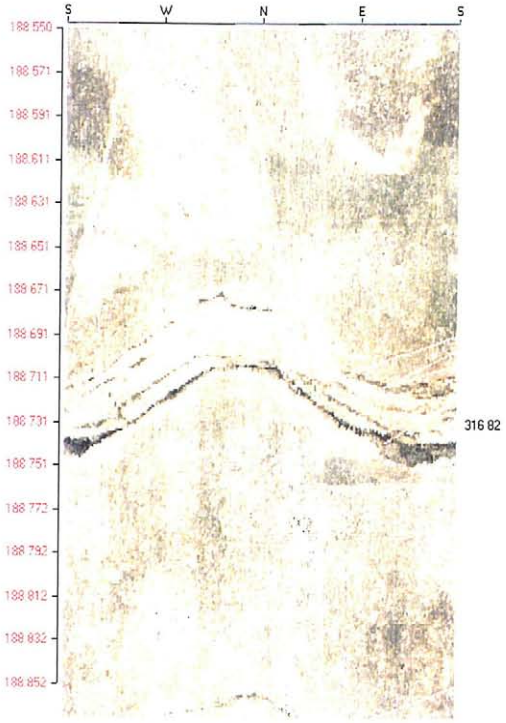

KA2563A
L = 188.7 m (316/82)

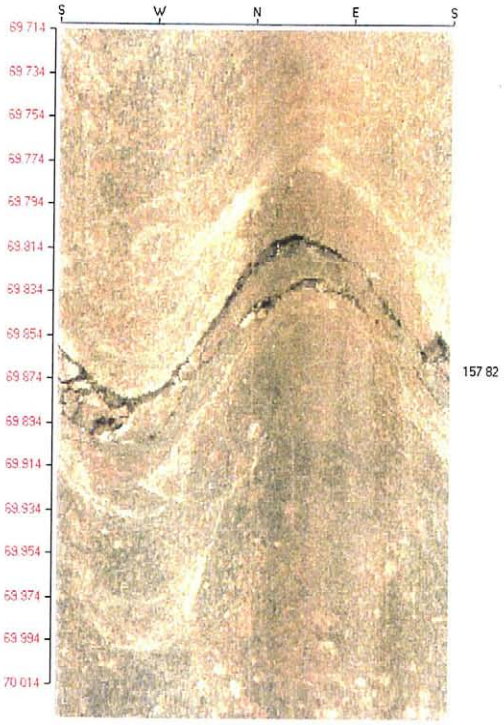

KI0023B
L = 69.8 m (157/82)

Structure #21

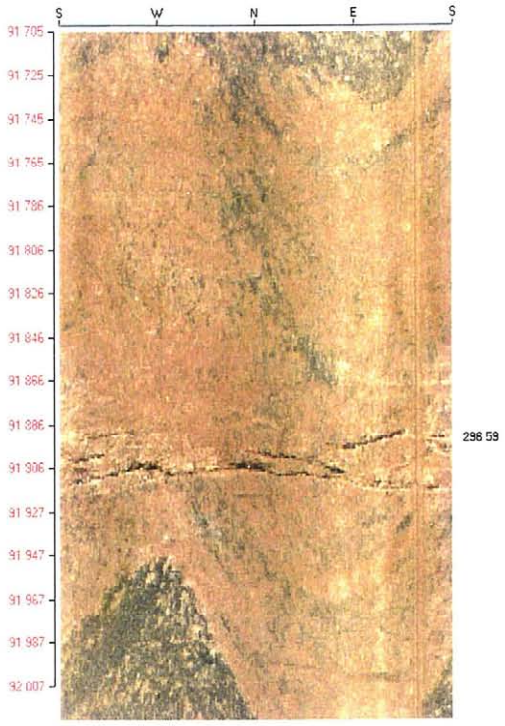

KI0025F03
L = 91.9 m (296/59)

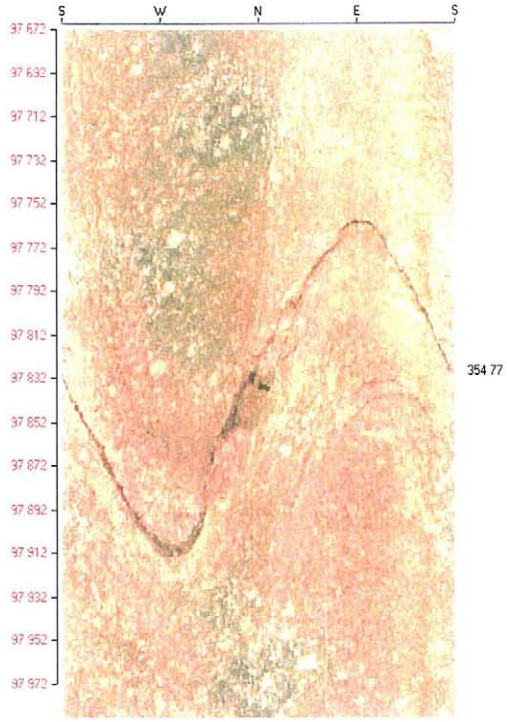

KI0025F02
L = 97.9 m (354/77)

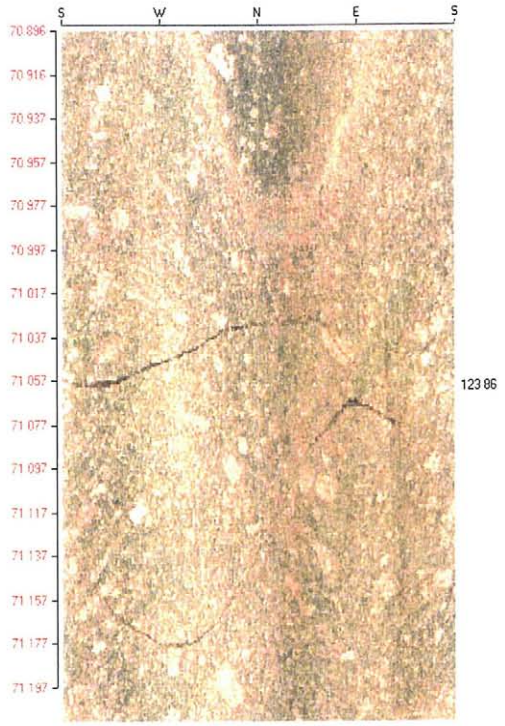

KI0023B
L = 71.1 m (123/86)

Structure #22

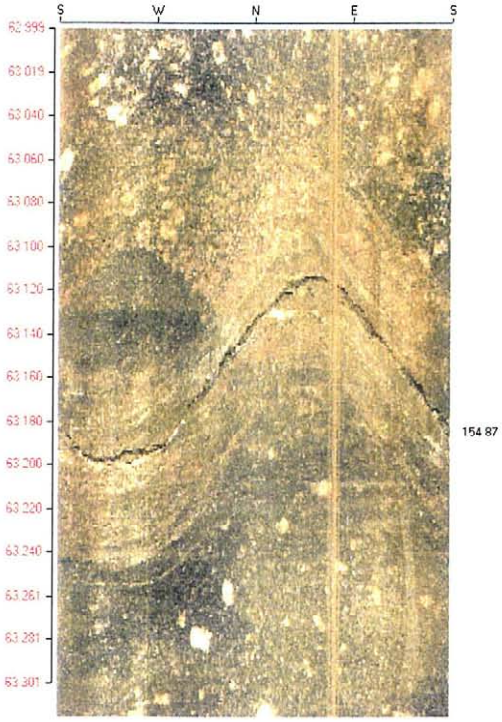

KI0025F03
L = 63.2 m (154/86)

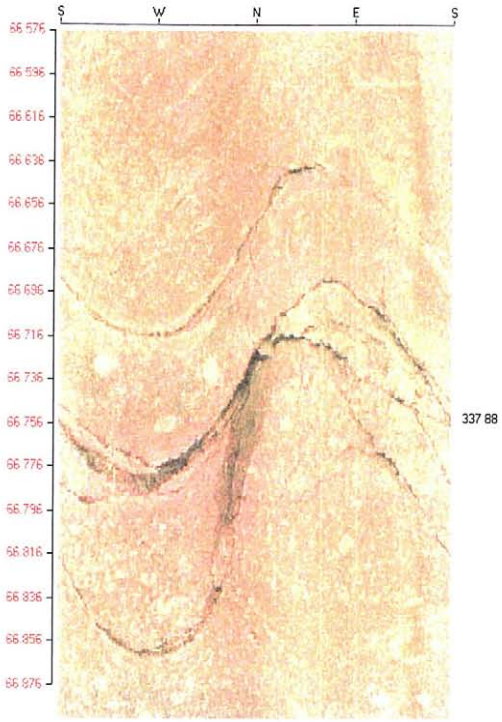

KI0025F02
L = 66.8 m (337/88)

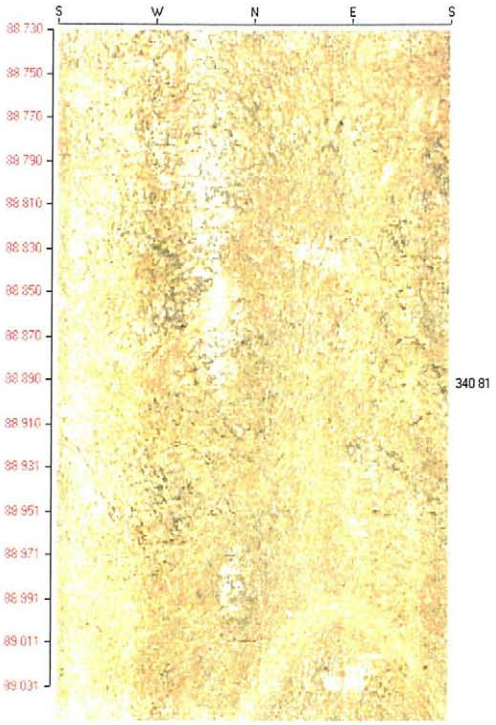

KI0025F
L = 88.8 m (340/81)

Structure in KI0023B

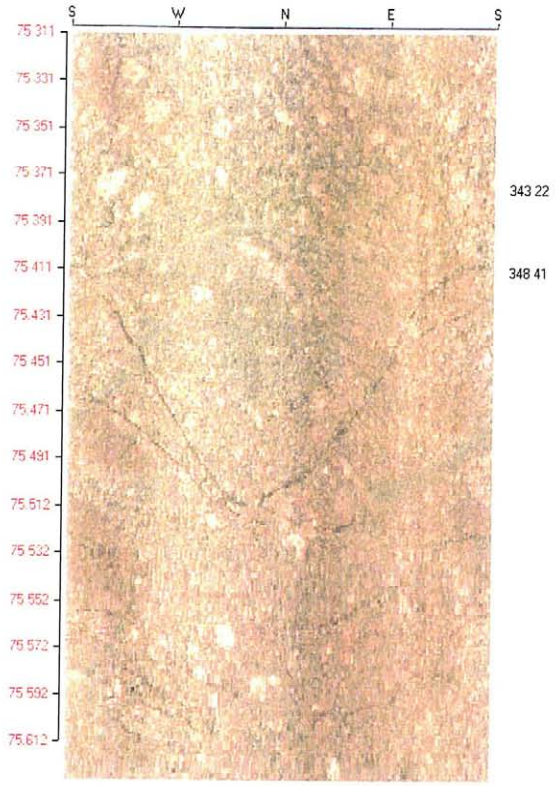

KI0023B
L = 75.5 m (348/41 alt 343/22)

Structure #23

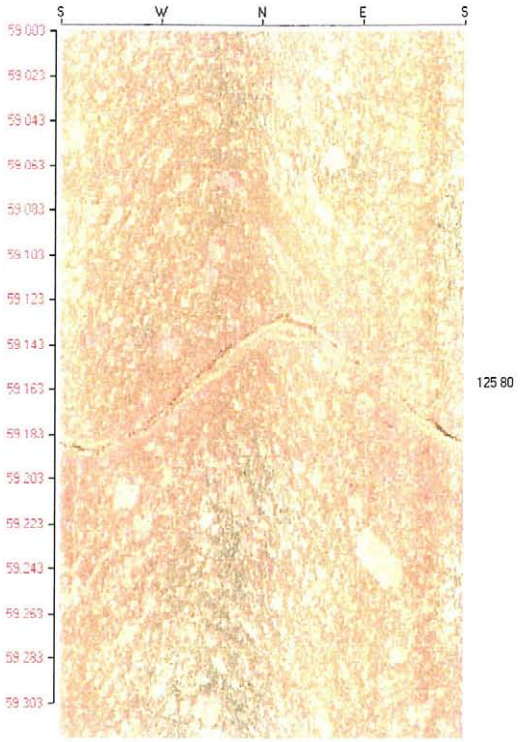

KI0025F02
L = 59.2 m (125/80)

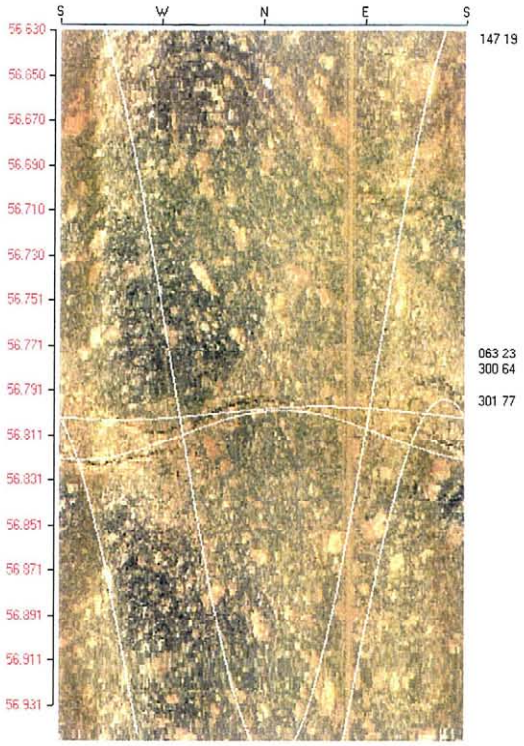

KI0025F03
L= 56.8 m (300/64 alt 301/77)

Structure #24

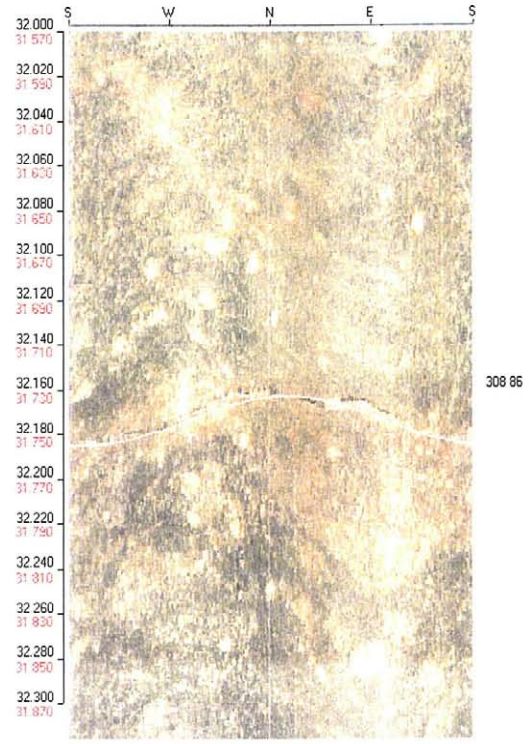

KI0023B
L = 31.75 m (308/76)

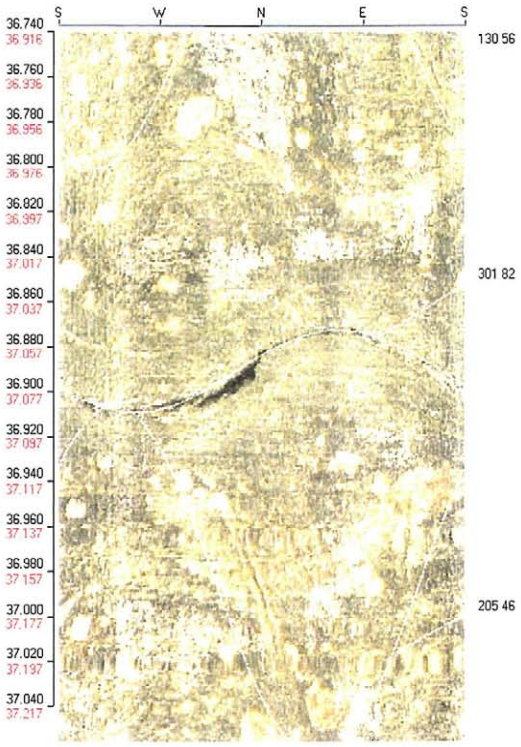

KI0025F
L = 37.1 m (301/82)

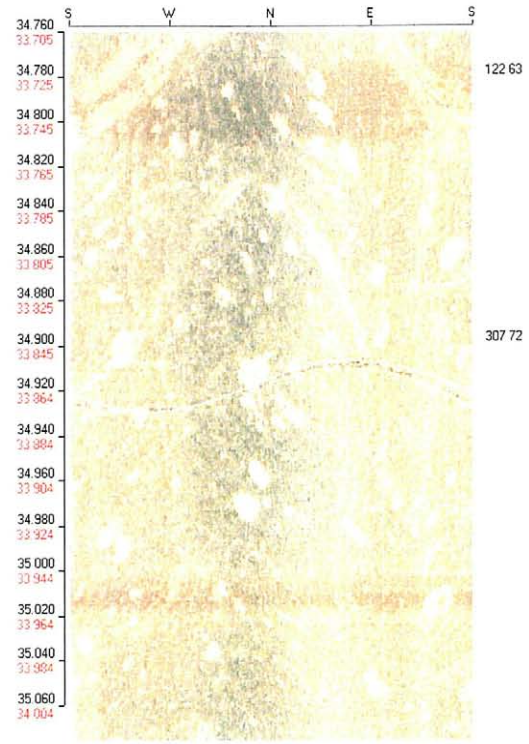

KI0025F02
L = 33.9 m (307/72)

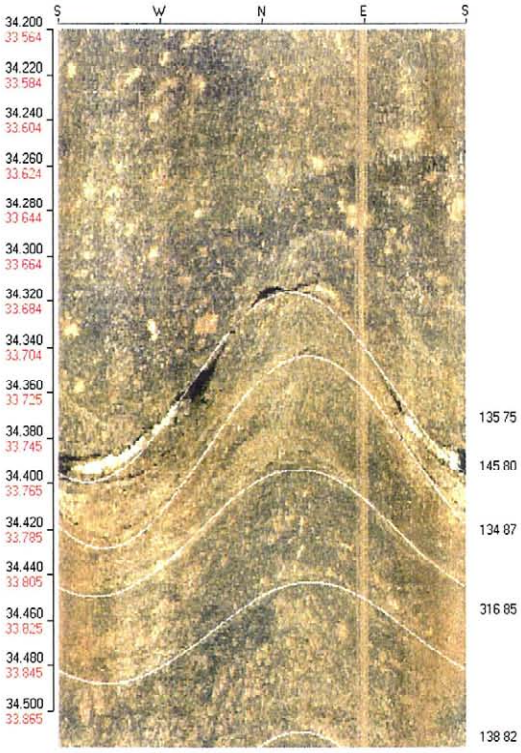

KI0025F03
L = 33.76 m (135/75)

Appendix C Supplementary figures

Appendix C- 1. KA2563A pressure responses to KI0025F03 drilling

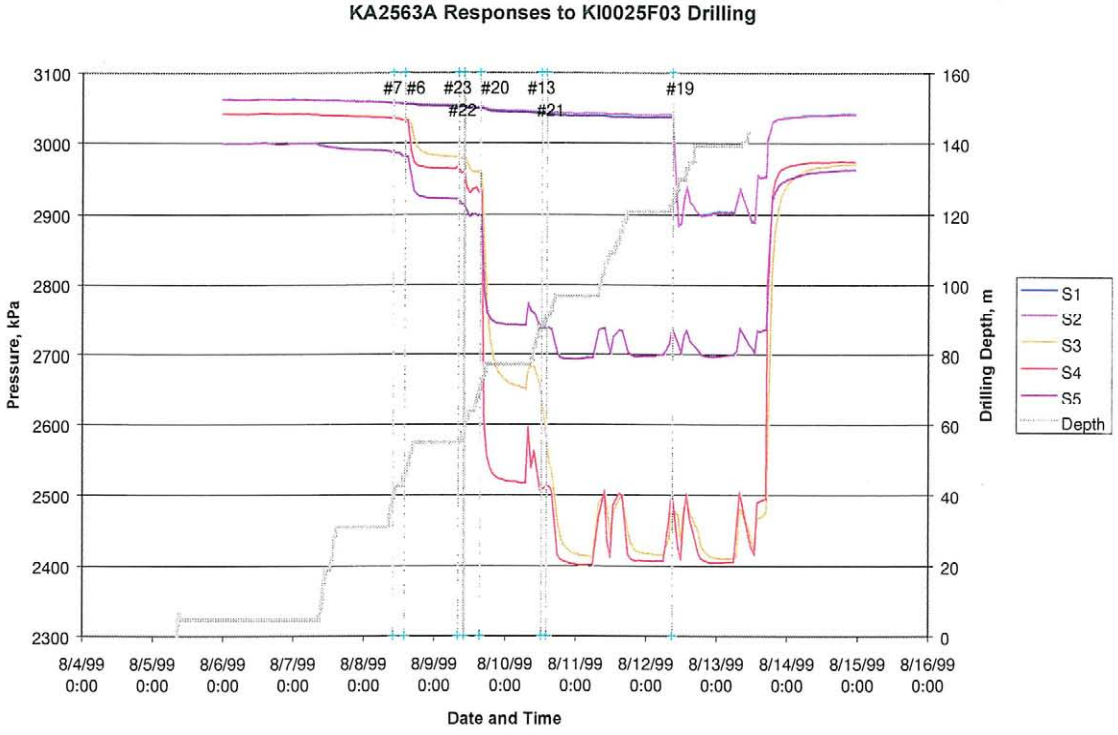

Appendix C- 2. KI0023B pressure responses to KI0025F03 drilling

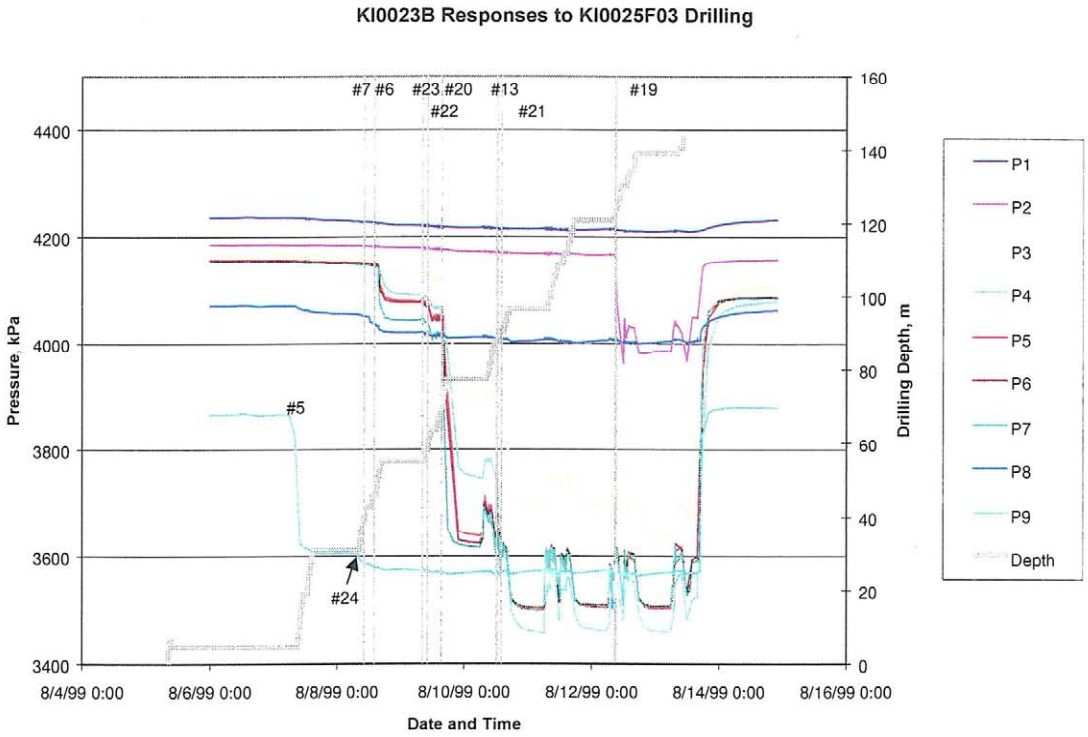

Appendix C- 3. KI0025F02 responses to KI0025F03 drilling

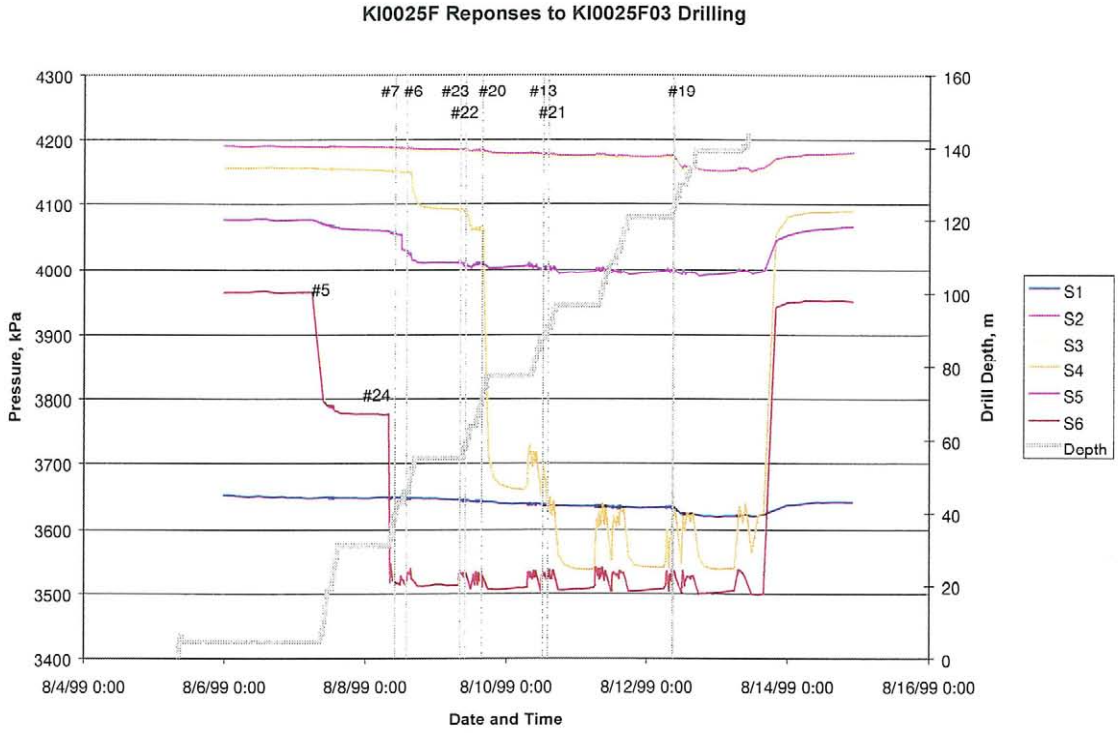

Appendix C- 4. KI0025F Responses to KI0025F03 drilling

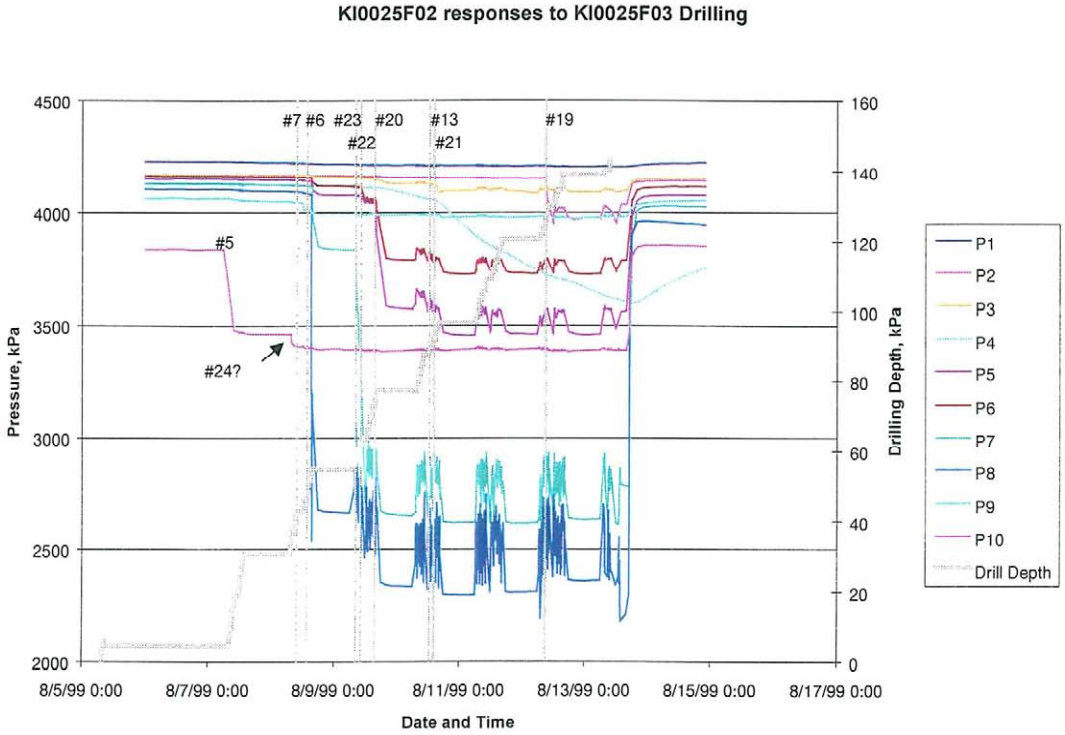

Appendix C- 5 Structure #6 in-plane map (based on Table 4-5 corners)

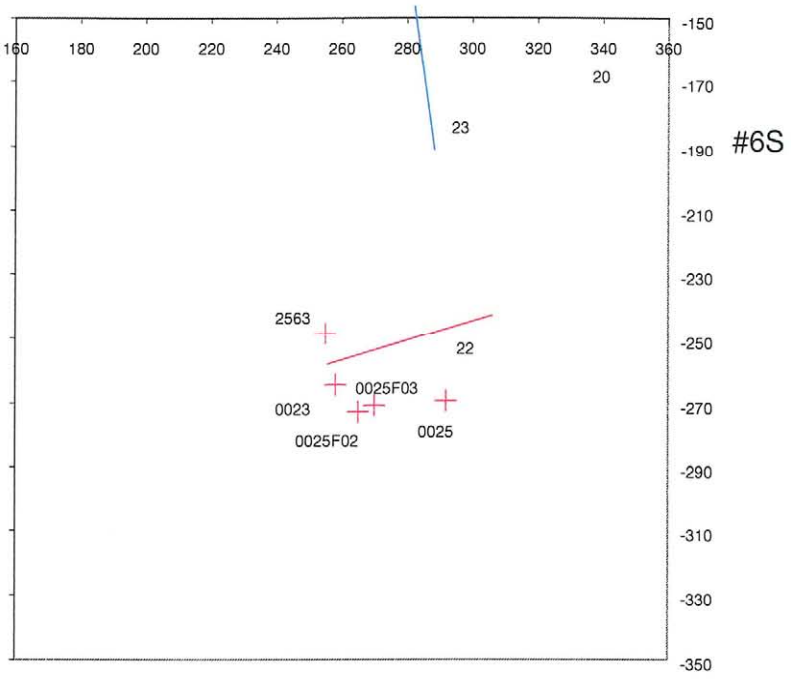

Appendix C- 6 Structure #23 in-plane map (based on Table 4-5 corners).

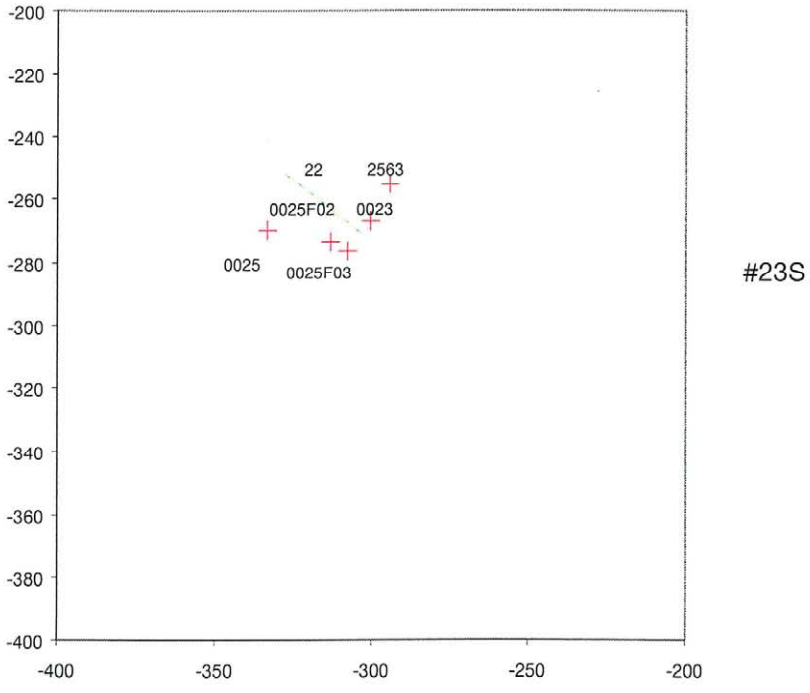

Appendix C- 7. Structure #22 in-plane map (based on Table 4-5 corners).

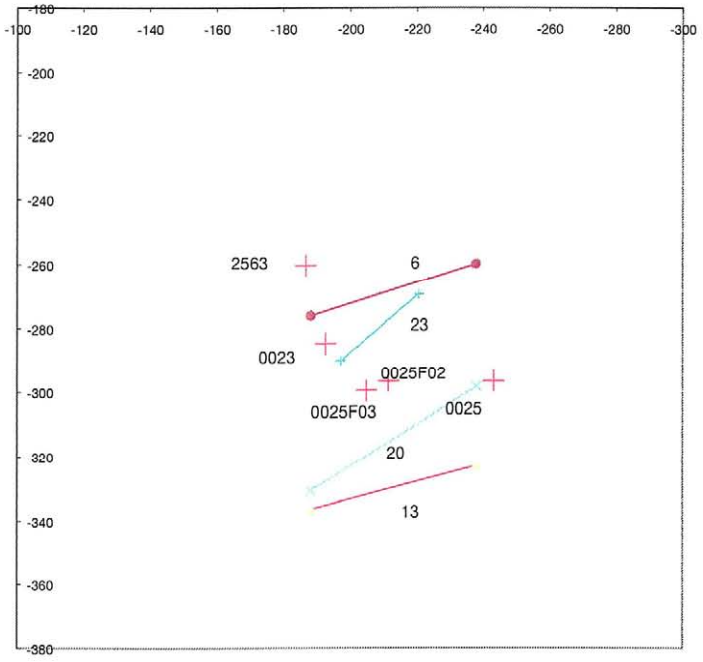

Appendix C- 8. Structure #20 in-plane map (based on Table 4-5 corners).

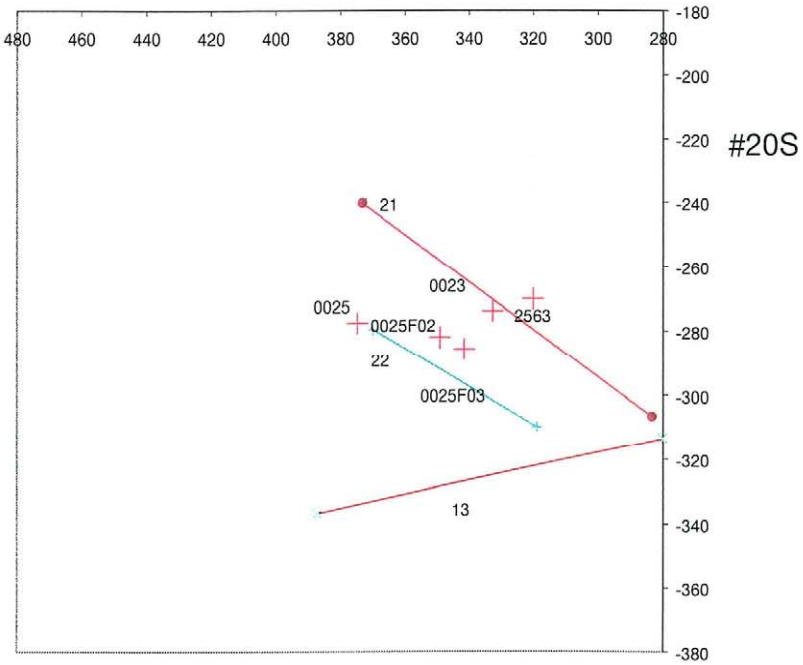

Appendix C- 9. Structure #13 in-plane map (based on Table 4-5 corners).

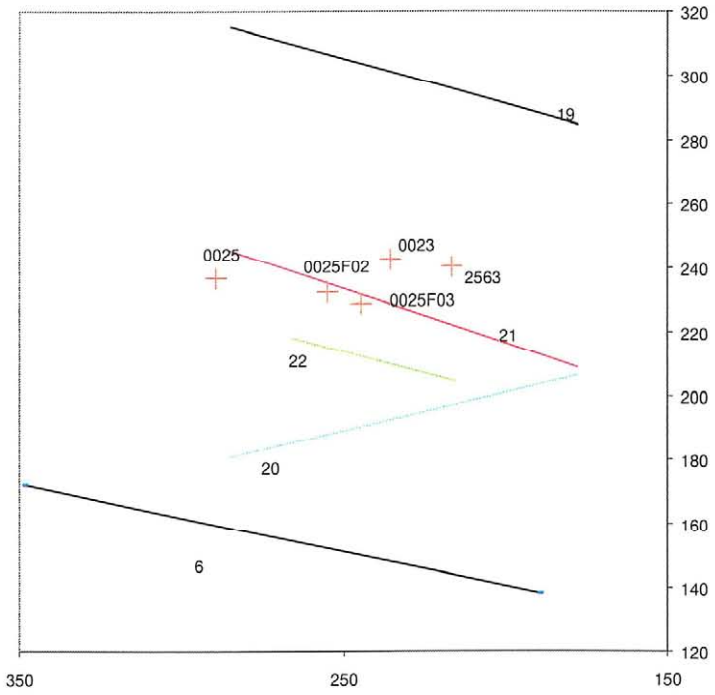

#13S

Appendix C- 10. Structure #21 in-plane map (based on Table 4-5 corners).

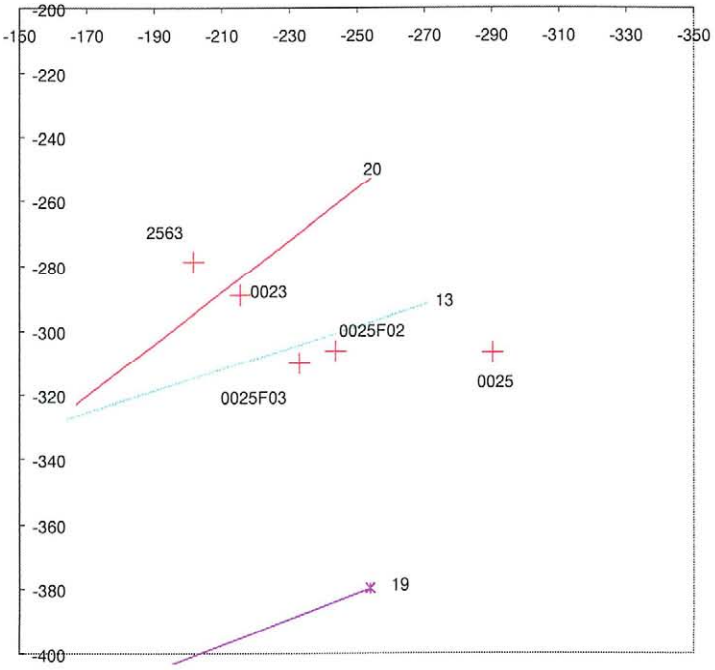

#21S

Appendix C- 11. Structure #19 in-plane map (based on Table 4-5 corners)

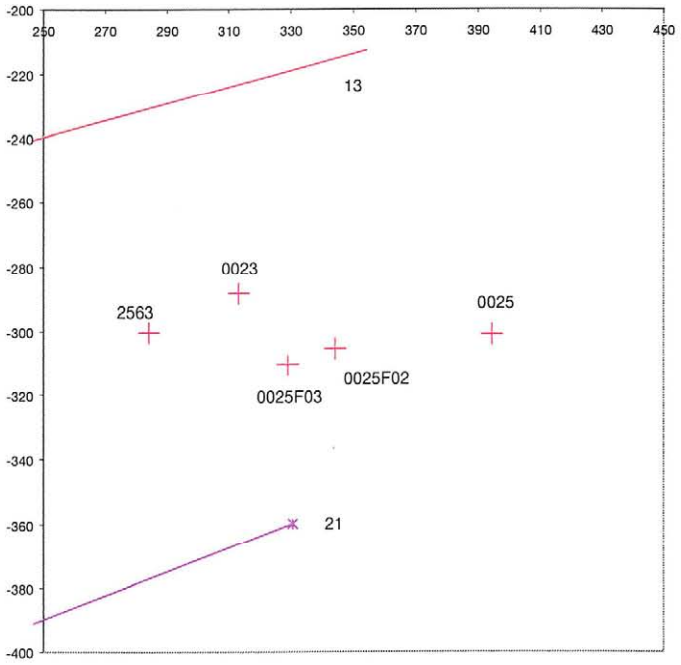

#19S